Biochemical Characterization of *Drosophila* Receptor Tyrosine Phosphatases

Thesis by

Bruce Seymour Burkemper

In Partial Fulfillment of the Requirements

for the Degree of

Doctor of Philosophy

California Institute of Technology

Pasadena, California

2003

(Defended February 4th, 2003)

Acknowledgments

I'm grateful for my good fortune in having had the privilege to be a member of the Caltech community. It has been immensely gratifying to be at an institution so renowned for its pursuit of excellence. Working among people who have not only a love of science, but minds keen enough to deal with its complexity has been a humbling experience. Of all the people I have worked with, two stand out as most embodying the spirit of Caltech, and they are the ones I would most like to thank. The first is my thesis advisor, Kai Zinn. Kai is the most erudite person I know, with an astounding memory and an uncanny ability for making astute observations. He also happens to be a skilled raconteur, so being in his company has always been interesting. I would very much like to thank him for his support and guidance, without which this thesis would not have been possible. I would also like to thank Peter Snow for applying his expertise in biochemistry to my projects. Peter lives for science, and it was very inspiring to work with someone with such dedication. The contributions made by him are the foundations upon which much of my thesis work is built.

Having a benevolent thesis committee has enriched my experience as a graduate student. I thank the members of my committee, Marianne Bronner-Fraser, Bruce Hay and Mary Kennedy, for taking an interest in my projects and giving me advice to help my work come to fruition.

Finally, I would like to acknowledge the generosity of the following people for their contributions: Corey Goodman (UC Berkeley) for Robo reagents, Paul Garrity (MIT) for the DA3 construct, Neil Kreuger (Harvard) for the DLAR construct, Gary Hathaway (Caltech PPMAL facility) for sequencing and mass spectrometry, Jody Franke and Dan Kiehart (Duke) for myosin II-tail-coated beads, and Liquin Luo (Stanford) for mushroom body reagents.

Abstract

Two classes of enzymes are responsible for modulation of intracellular phosphotyrosine levels, namely protein tyrosine kinases (PTKs) and protein tyrosine phosphatases (PTPs). Together these enzymes maintain the appropriate balance of phosphoproteins required for a variety of developmental processes including axon pathfinding. In *Drosophila*, five receptor-like protein tyrosine phosphatases (RPTPs) regulate axon pathfinding, but little is known about their downstream signaling pathways or the means by which their enzymatic activity is regulated.

Chapter 2 of this thesis deals with experiments to test whether dimerization regulates the activity of these enzymes. Crystallographic data indicates that some RPTPs form dimers in which each monomer is precluded from binding substrate due to the insertion of a helix-turn-helix segment of the opposing monomer into the active site. I introduced "tagged" RPTP constructs into *Drosophila* S2 tissue culture cells and tested for dimer formation using immunoprecipitation and Western blotting. I did not detect stable dimers, however. This may suggest that dimer formation requires other protein components (such as the putative RPTP ligands) that are not expressed in S2 cells.

In Chapter 3 I investigated the possibility that Roundabout (Robo), a receptor mediating axonal repulsion from the embryonic midline, is a substrate for RPTPs DPTP69D and/or DPTP10D. Previous genetic studies implicate these RPTPs in participating in the Robo signaling pathway. Experiments detailed here show that Robo can be phosphorylated on tyrosine residues in S2 cells, characteristic of an RPTP substrate. However, Robo did not co-immunoprecipitate with "substrate trap" mutants of either of these RPTPs, possibly because their interaction is dependent on co-factors not present in the cell culture system.

Chapter 4 is a characterization of DPTP69D-associated proteins purified from embryos expressing a substrate trap version of DPTP69D. We identified one of the associated proteins as non-muscle myosin II heavy chain (nmm II hc). Proper regulation of nmm II hc is essential for axon patterning in mushroom bodies (MBs). I found that expression of the DPTP69D trap in MBs results in an axon retraction phenotype similar

to that seen when nmm II hc activity is elevated, suggesting that this protein may be a target for DPTP69D activity.

Table of Contents

Chapter 1

Structure and function of receptor tyrosine phosphatases

Introduction

The evolutionary transition from unicellular to multicellular organisms was predicated on the development of a mechanism for cell-cell signaling. Transmembrane signaling events underlie a myriad of developmental processes including morphogenesis, pattern formation and differentiation. The adult multicellular organism is also dependent on cell-cell signaling for many aspects of normal cell maintenance and functioning. A variety of extracellular stimuli such as cytokines, growth factors and hormones activate receptor protein tyrosine kinases (PTKs) leading to an increase in intracellular phosphorylation levels. PTKs are also activated through various types of cell-cell, cell-matrix interactions. The resulting phosphorylation of select intracellular target proteins triggers downstream signaling pathways that effect diverse responses through generation of second messengers and activation of other proteins, such as Ser/Thr kinases and G-proteins.

Tyrosine phosphorylation is a viable means of manifesting cell-cell signaling only if the phosphorylation is reversible. In general, once a given signal has caused it to increase, the level of intracellular phosphotyrosine must return to a baseline in order for the cell to respond to subsequent signals. Equally important as PTKs, then, are the protein tyrosine phosphatases (PTPs) that subserve this function. Similar to PTKs, the importance of these enzymes is reflected in their diversity. PTPs can be grouped into two structurally distinct groups: receptor-like proteins that span the membrane and soluble cytosolic enzymes. Receptor-like protein tyrosine phosphatases (RPTPs) have the potential to transduce extracellular signals into changes in phosphotyrosine levels via ligand binding-induced activation of their catalytic domain. Instead of simply reversing phosphorylation mediated be kinases, RPTPs may play an active role in regulating the cellular response to outside signals.

In the following sections I will review our current knowledge of the RPTPs. (1) Certain residues are highly conserved in the RPTP catalytic domain and known to be essential for catalytic activity. Our current understanding of the basic enzymatic mechanism for RPTPs is supported by a large body of empirical evidence. Elucidation of this mechanism has contributed to the development of mutant trap versions of these

enzymes that have been useful in identifying potential RPTP substrates. (2) RPTPs have well-defined preferences for substrates. It has been shown that protein tertiary structure is not as important as the primary sequence adjacent to the phosphotyrosine residue in determining the suitability of a given phosphopeptide as a substrate. (3) Interactions within and between RPTPs are an important means by which the activity of these enzymes is regulated. In particular, the “wedge” region plays a critical role in extinguishing enzymatic activity. (4) With few exceptions, RPTPs have two catalytic domains, D1 and D2. Most activity resides in D1, but the low level of activity in D2 can be increased to levels comparable to D2 through mutation of just two residues.

1. Enzymatic mechanism

All “classical” tyrosine phosphatases have a conserved catalytic domain of approximately 240 residues characterized by the PTP signature motif (I/V)HCXAGXXR(S/T)G. This motif contains invariant cysteine (Cys) and arganine (Arg) residues that are essential for catalytic activity. The role of the Arg is to assist in positioning the phosphotyrosine substrate (pTyr) such that its phosphorus atom is situated adjacent to the sulfur atom of the PTP motif’s catalytic Cys residue (Jia et al., 1995). This allows Cys to launch a nucleophilic attack on the phosphorus atom, the first step in the dephosphorylation reaction.

The PTP motif is situated near the center of the molecule and is surrounded by four loops that delineate the entrance to the active site: L1, L6, L13 (or WpD) and L17. Binding of substrate results in a conformational change in the WpD loop from an open position into a catalytically competent closed position. This brings the side chain of an invariant, catalytically essential aspartic acid on the loop (Asp 181 in PTP1B) into position to act as a general acid. The closed WpD conformation is stabilized by a combination of hydrogen bonds and hydrophobic interactions.

Attack of the Cys nucleophile on phosphorus results in a pentavalent transition state. In donating a proton to this transition state, Asp 181 helps to cleave the P-O bond between the phosphorus and the oxygen of the tyrosyl side chain in the substrate. The result is formation of a thiol-phosphate (phosphoenzyme) intermediate.

The final step in the dephosphorylation reaction is hydrolysis of the thiol-phosphate intermediate by an activated water molecule. A glycine residue in the PTP facilitates this step by positioning the nucleophilic water molecule adjacent to the phosphorus atom of the intermediate. Gln 262 participates in hydrogen bonding with the water molecule to give it the proper orientation. Next, the same Asp that earlier served as a proton donor now acts as a proton acceptor and abstracts a hydrogen from the water molecule. This converts it into an active nucleophile that attacks the phosphorus atom, thereby cleaving the cysteinyl-phosphorus bond and reconstituting the enzyme. A schematic of the PTP dephosphorylation reaction is shown in Figure 1.

Several lines of evidence support this mechanism of catalysis. Site directed mutagenesis of the catalytic Cys results in an inactive phosphatase in an assay with 32P-labeled substrates (Guan and Dixon, 1991). When the invariant Asp is mutagenized, there is a marked reduction in catalytic activity (Zhang et al., 1994b) and substrates remain bound to the enzyme (Flint et al., 1997). The latter finding is consistent with the proposed role of Asp in cleaving the pTyr P-O bond that would cause release of the dephosphorylated substrate. We have exploited the substrate trapping properties conferred by this mutation in a search for RPTP substrates (see Chapters 3 and 4). Finally, substitution of Gln 262 for Ala leads to accumulation of the thiol-phosphate intermediate, consistent with the role of this residue in catalyzing hydrolysis of the intermediate (Denu et al., 1996).

2. Substrate binding

Several criteria determine the suitability of a given protein as a substrate for PTPs. The most important is that it is phosphorylated on one or more tyrosine residues. PTPs display a rigid specificity for pTyr-containing substrates, and proteins phosphorylated on other residues are unable to be dephosphorylated by these enzymes. This distinguishes the PTPs from Ser/Thr phosphatases and the dual-specificity phosphatases, the latter being able to dephosphorylate proteins phosphorylated on Ser, Thr and Tyr residues.

To determine the other criteria for PTP substrates, phosphorylated synthetic peptides are commonly used as model substrates. This approach is more practical than

using physiological substrates because few naturally occurring pTyr-containing substrates are readily available. Also, the broad specificity of kinases can be exploited to phosphorylate a diverse collection of artificial peptide substrates in vitro. For example, a series of peptides differing by just one residue can be kinased and tested with a PTP to determine the relative importance of each residue in the peptide for the dephosphorylation reaction.

Dimensions of the catalytic site cleft are the primary determinant of the molecular basis for PTP substrate specificity (Dunn et al., 1996). The nucleophilic Cys is situated at the base of this cleft, and there is a distance of 9 Aº from it to the cleft entrance. A conserved KNRY sequence forms a phosphotyrosine recognition loop that contributes to formation of the cleft (Jia et al., 1995). The Tyr residue from this loop and other nonpolar residues from the WpD loop interact with the phenyl ring of the substrate peptide's pTyr. These interactions cause the pTyr residue to adopt a helical conformation that inserts into the cleft. The importance of the cleft's depth was documented in experiments with a peptide of the general form $(Glu)_4$-NH-$(CH_2)_n$-PO_3. The peptide that was most efficiently dephosphorylated was the one where n=7, which corresponds exactly to the length of a tyrosine residue.

Studies of several PTPs have determined that pTyr site recognition depends not on higher orders of protein conformation but on the primary sequence surrounding pTyr, particularly amino acids immediately N- and C-terminal to this residue. For a particular pTyr-containing substrate, the rate of dephosphorylation by PTP can be easily measured with a continuous spectrophotometric assay due to the different absorption spectra of pTyr versus Tyr. Several PTPs have been examined with this assay to define precisely which substrate residues are important for efficient dephosphorylation.

In the case of PTP1 and Yersinia PTPase, four residues N-terminal and one residue C-terminal to pTyr were found to be key determinants of substrate suitability (Zhang et al., 1994a). This was determined by sequentially substituting Ala for each amino acid within a pTyr-containing peptide substrate derived from the EGF receptor ($EGFR_{988-998}$: DADEpYLIPQQG), and measuring the kinetics of the dephosphorylation reaction. The -1 position immediately N-terminal to pTyr was found to be particularly important, as a substitution of the Glu residue here for Ala resulted in a 126-fold decrease in enzyme

activity on this peptide compared to wild-type peptide. Additional experiments with various length substrates determined that a minimum of six amino acids is required for optimal binding to these PTPs, including the pTyr residue.

In general, PTPs have a documented preference for substrates with acidic residues N-terminal to the pTyr due to the presence of basic residues on the PTP surface that interact with these residues. The presence of pTyr is necessary but not sufficient for high-affinity binding to PTPs, as a singular pTyr residue binds only weakly, and peptides without pTyr do not bind at all (Barford et al., 1998).

3. Modulation of activity

Regulation of intracellular phosphorylation levels is a fundamental mechanism used by cells to regulate a wide array of cellular functions including proliferation, differentiation and metabolism. In axon patterning, RPTP activity is required at specific points along the path of extending axons to keep them oriented towards their target. It is clear that the involvement of PTPs in these processes requires that their activity be specifically regulated. This is accomplished in some measure through proteins that target the enzymes to specific subcellular locations. Other mechanisms of regulation have yet to be discovered.

PTPs are efficient catalysts, and isolated catalytic domains exhibit constitutive activity. The pathogenicity of the Yersinia bacteria responsible for tuberculosis and bubonic plague is due to disruption of signal transduction pathways resulting from constitutive activity of the Yop family PTPs that it injects into macrophages. Thus, regulation of PTP activity may come in the form of inhibition of their activity.

Dimerization has been proposed as one means by which PTP activity may be inhibited. The first evidence supporting this theory comes from crystallographic studies of RPTPα. Like most phosphatases, RPTPα consists of two catalytic domains, D1 and D2, each with an active site. The crystal structure of the first catalytic domain indicates a region of each catalytic domain, denoted the “wedge,” inserts into the active site of the neighboring RPTPα molecule (Bilwes et al., 1996). These results suggest that dimer formation may represent a way of reversibly suspending phosphatase activity, as a

blocked active site would preclude substrate binding. In this scenario, RPTPs would be active only when they have been dissociated from dimers into monomers (Figure 2).

The wedge of RPTPαD1 is formed from a helix-turn-helix segment in the N-terminal segment of each monomer. The interhelical angle is ~80º, forming a wedge that inserts into the catalytic cleft of the opposing monomer. Hydrogen bonds and van der Waals interactions between the N-terminal wedge of one monomer and residues from the WpD loop of its dimer partner stabilize the WpD loop in the open conformation. This prevents the loop from moving into the catalytically competent closed position. Additionally, the side chains of several N-terminal wedge residues interact with residues Tyr 262 and Asn 264 on the L1 loop of the opposite dimer. These are the equivalent of residues Tyr 46 and Asp 48 in PTP1B, two residues that have been shown to form critical interactions with the pTyr-containing substrate. This suggests dimerized RPTPαD1's are incapable of binding substrate.

Taken together, the crystallographic data indicate that activity is proscribed in the dimeric form of RPTPαD1 on several levels. The catalytic site is physically occluded by the wedge, an Asp on the WpD loop essential for activity is kept away from the active site by interactions holding the loop in an open conformation, and residues that participate in substrate binding are otherwise engaged in interactions with the L1 loop. The sequences corresponding to the wedge show a high degree of conservation among other RPTP family members, suggesting that dimerization as a means of activity regulation could be a strategy common to many RPTPs.

Additional evidence for a model of dimer formation as a means of reversibly suspending RPTP activity comes from studies of an EGFR/CD45 chimera (Desai et al., 1993; Majeti et al., 1998). CD45 is an RPTP with no known ligand that is expressed on nucleated hematopoietic cells and is required for TCR signaling in response to engagement of antigen receptor. To study the effects of dimerization on CD45 activity, a chimeric protein was made with the extracellular and transmembrane domains of EGFR fused to the intracellular domain of CD45. TCR signaling is normal in cells expressing the chimeric protein, but addition of EGF results in an abrupt loss of signaling. Signaling is restored in the presence of EGF when the chimera is coexpressed with a gene encoding only the extracellular and transmembrane portions of EGFR. These results suggest that

induced dimerization extinguishes the catalytic activity of the chimeric protein. Under physiologic conditions, ligand may substitute for EGF in inducing dimerization of wild-type CD45. Consistent with this, the wedge domain of CD45 is highly conserved with that of RPTPα, suggesting it may form dimers in a manner similar to RPTPα.

Other studies have shown dimer interactions can be complex, with a domain from one RPTP inserting into the catalytic domain of a different RPTP to form cross-species heterodimers (Blanchetot and den Hertog, 2000; Gross et al., 2002). For example, the second catalytic domain (D2) of PTPδ has been shown to bind to D1 of RPTPσ, and this results in ~50% reduction in catalytic activity of the latter (Wallace et al., 1998). Evidence also exists for formation of multimers, where strings of RPTPs are interconnected via interactions between wedge and active site domains of neighboring molecules (Iversen et al., 2002).

Strong evidence exists for a model of negative regulation of activity through dimerization for the RPTPs cited above, but the crystal structures of some other RPTPs suggests this is not a universal strategy employed by all RPTP family members. For example, RPTPμ does exist as a dimer in the crystal structure, but the wedge domain of one subunit of the dimer is not inserted into the catalytic cleft of the dyad-related monomer. Consequently, the active site remains in an open, uninhibited conformation (Hoffmann et al., 1997). In the case of RPTP LAR there is no direct evidence for a dimer, but other types of intramolecular interactions are thought to occur. The crystal structure suggests D1 of one LAR molecule may interact with D2 of a second molecule (Nam et al., 1999).

4. D1 vs. D2

Most RPTPs have two tandem phosphatase domains denoted D1 and D2. Studies of human RPTP LAR indicate the tertiary structure of LAR D1 and D2 are very similar (Nam et al., 1999). However, as is the case with other RPTPs, a majority of the catalytic activity resides in the membrane-proximal D1, with membrane-distal D2 possessing little or no activity. This raises two questions that apply to all members of the RPTP family: 1) what accounts for the disparity in catalytic activity between D1 and D2, and 2) if D2 is

not catalytically active, what function(s) does it serve? The high degree of primary sequence conservation among RPTP D2 domains suggests there does exist an as yet undiscovered function.

The most obvious difference between LAR D1 and D2 is the presence of four additional residues in D2 located in the loop between helices α1' and α2'. Alignment with sequences of other RPTPs shows the extra residues are shared by many D2 domains, suggesting the longer loop resulting from these additional residues may have biological significance.

Overall similarity is observed in the active site of both domains, each comprised of a catalytic cleft surrounded by four loops. Closer inspection reveals a substitution of two amino acids with important roles in the catalytic reaction. In PTP1B, an Asp on the WpD loop is thought to act as a general acid when the loop assumes the catalytically competent closed conformation. By donating a proton to the tyrosyl oxygen, Asp 181 assists in the reaction by turning the soon-to-be dephosphorylated substrate into a favorable leaving group. In D2 of LAR, the residue equivalent to Asp 181 is replaced by Glu 1779. The second substitution is found in the pTyr recognition loop that has been shown to interact with the substrate pTyr. In PTP1B, Tyr 46 forms hydrogen bonds with the Ser residue immediately adjacent to the catalytically essential Cys. The LAR residue corresponding to Tyr 46 is Leu 1644, which does not participate in hydrogen bonding with Ser. The absence of this interaction causes Ser to shift slightly into the path of the catalytic cleft, thereby precluding potential substrates from gaining access.

Mutational analysis was performed to determine whether these amino acid substitutions were responsible for the lack of phosphatase activity in D2. Individual substitutions of Glu 1779 for Asp or Leu 1644 for Tyr resulted in detectable dephosphorylation of a 32P-labeled synthetic peptide, but the level of activity was a small fraction of that of wild-type enzyme. When both substitutions were made together, a far greater impact was observed, with D2 now showing activity levels equivalent to that of D1. Conversely, when the Asp and Tyr residues of D1 are mutated, D1 catalytic activity is abolished. Thus, the difference in catalytic potential of these domains is accounted for in its entirety by only these two residues.

Amino acid substitutions that correspond to those made in LAR D2 also result in fully restored activity of the D2 domain of RPTPα , suggesting this is a common means for D2 inactivation (Lim et al., 1998). Although the D2 domain plays little or no role in catalysis, the high degree of sequence conservation among RPTP family members suggests they do have an important function. One possibility is that D2 is involved in regulating the substrate specificity of D1. Consistent with this, the N-terminal part of LAR D2 interacts with D1 via hydrogen bonds and van der Wall forces and forms a wall on one side of the D1 active site. Mutants missing the N-terminal part of D2 show altered substrate specificity, while no such effect is seen in mutants in which the C-terminal part is missing. A similar observation has been made in the case of CD45, where a 19 residue insertion between two β sheets of the D2 domain results in altered D1 specificity for synthetic peptides (Streuli et al., 1990).

D2 domains may also be important for substrate binding, with evidence in support of this role provided by studies with insulin receptor (IR), a physiological LAR substrate (Tsujikawa et al., 2001). LAR constructs missing either the D1 or D2 domain were coexpressed with IR in COS cells. Following addition of insulin to stimulate IR autophosphorylation, LAR was immunoprecipitated (IPd) with an antibody against its extracellular domain. IR co-IPd efficiently with constructs missing the D1 domain, but the amount co-IPing with constructs missing the D2 domain was negligible.

Figure 1. Schematic of the reaction mechanism catalyzed by PTP1B. (a) Formation of the cysteinyl-phosphate intermediate. (b) Hydrolysis of the cysteinyl-phosphate intermediate.

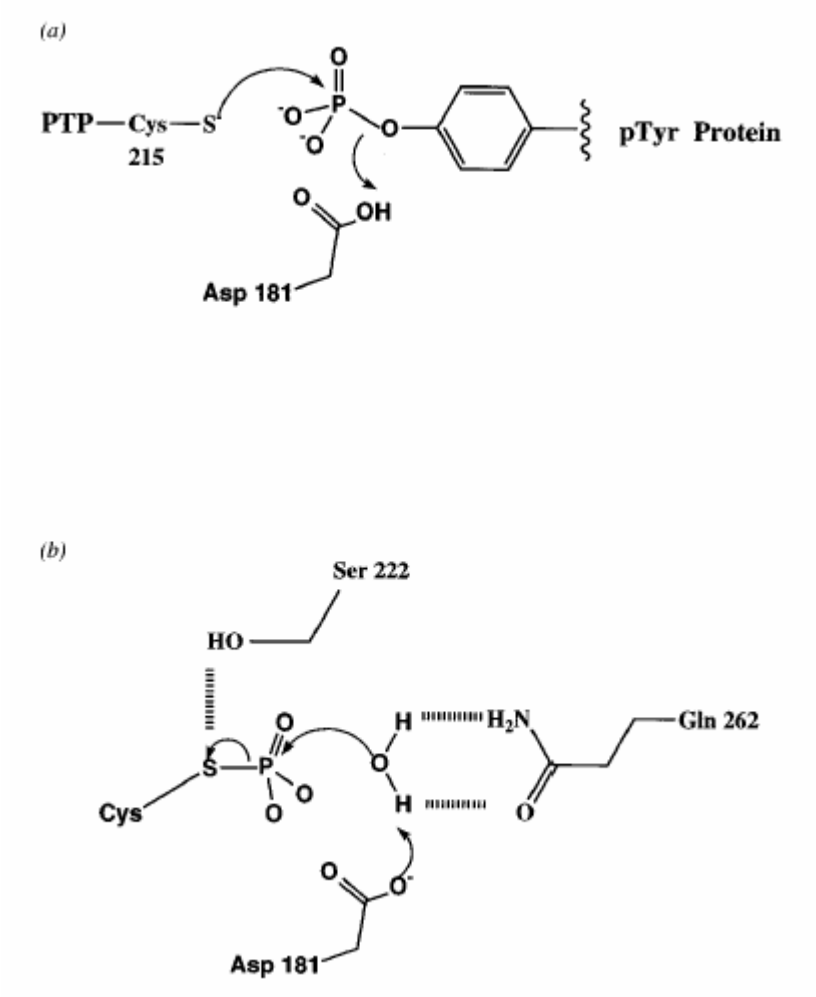

Source: Annual Review of Biophysics and Biomolecular Structure (1998) **27**, 154

Figure 2. Stereo ribbon diagram of the RPTPαD1 dimer. The label AS placed near the catalytically essential Cys 433 emphasizes the active site of each monomer.

Source: Nature (1996) **382**, 556

Chapter 2

Analysis of RPTP dimerization potential in *Drosophila* S2 cells

Abstract

The vital role of receptor-linked tyrosine phosphatases (RPTPs) in *Drosophila* axon pathfinding has been well documented, yet little is known about how the activity of these enzymes is regulated. Crystallographic data suggests activity may be regulated through dimerization, as the “wedge” domain of one RPTP appears to insert into the active site of its dimer partner, thereby precluding it from binding substrate. Genetic data from our lab provides corroborating evidence for a model of dimer mediated regulation of activity. To assay for dimer formation, we expressed affinity-tagged versions of the RPTPs in the *Drosophila* S2 cell line. No evidence for stable dimers was found under the conditions tested, possibly because dimer formation is ligand induced. Our experimental approach can be used to study the role of ligands in inducing RPTP dimerization once such ligands are identified.

INTRODUCTION

The process of axon guidance requires the maintenance of an appropriate balance of intracellular tyrosine phosphorylation levels, which is maintained by two classes of enzymes: protein tyrosine kinases (PTKs) and protein tyrosine phosphatases (PTPs). Each class is comprised of a large family of multidomain proteins in both cytoplasmic and transmembrane receptor forms. Many receptor-linked tyrosine phosphatases (RPTPs) resemble cell adhesion molecules in that their extracellular domains consist of fibronectin type III (FN III) repeats and/or immunoglobulin-like (Ig) domains. This suggests RPTPs may be one means by which cell recognition events are coupled to changes in cytoplasmic phosphorylation levels.

In *Drosophila*, five RPTPs have been identified that play a role in axon pathfinding. DPTP69D, DPTP10D, DPTP99A, DLAR, and DPTP52F are exclusively expressed in CNS neurons during the period of axonogenesis, and flies with mutations in their genes show characteristic defects in axon guidance during embryonic development (Desai et al., 1996; Desai et al., 1997; Krueger et al., 1996; Schindelholz et al., 2001; Sun et al., 2000; Sun et al., 2001). Four of the five RPTPs (DPTP69D, DPTP10D, DPTP99A and DLAR) are restricted to axons. An axon reaches its target by taking a series of steps past intermediate targets, each successive target leading it closer to its final destination. The intermediate targets, called choice points, are places at which the axon makes a decision about the trajectory it will follow in the next segment of its journey. Modulation of RPTP activity at these points is thought to be required for changes in growth trajectories. Successful navigation past a series of choice points to an end target thus depends on the coordinated regulation of these proteins. Despite extensive studies documenting the pathfinding role played by the RPTPs, little is known about how their activity is regulated.

Crystallographic studies of mammalian RPTPs suggest that dimerization may regulate the activity of these enzymes (Jiang et al., 1999). Like most transmembrane phosphatases, RPTPα has two catalytic domains, D1 (membrane-proximal) and D2 (membrane-distal), each with an active site. The crystal structure for this protein indicates that a region of each D1 catalytic domain, denoted as the “wedge,” inserts into the active site of the neighboring RPTPα molecule (Bilwes et al., 1996). These results suggest that

dimer formation may represent a way of reversibly suspending phosphatase activity, as a blocked active site would preclude substrate binding. In this scenario, RPTPs would be active only when they have been dissociated from dimers into monomers. Signals present in the environment traversed by the axon during extension may serve to bring RPTP monomers together to temporarily extinguish their activity. Similarly, other signals may work to cause existing dimers to dissociate into monomers, thereby switching activity on. A combination of these signals, at the appropriate time and place during axonogenesis, could play a central role in facilitating the navigation of axons to their targets.

Several considerations make regulation of *Drosophila* axonal RPTPs through dimerization an appealing model worth testing. First, four RPTPs (DPTP10D, DPTP69D, DPTP99A, DLAR) have sequences similar to the wedge found in RPTPα (Figure 1). Second, previous work in the lab has revealed that a heteromultimer including DPTP10D and DPTP69D is capable of forming. Third, genetic data gathered in our lab indicates that DLAR suppresses the activity of DPTP99A (Desai et al., 1997). One way to explain this result is to invoke formation of a DLAR/DPTP99A heterodimer. Finally, a precedent for activity modulation through dimerization exists in RPTP counterparts, namely receptor tyrosine kinases (RTKs).

We tested the dimerization model by cotransfecting epitope-tagged RPTP expression constructs pairwise into *Drosophila* S2 cells, immunoprecipitating one and looking for evidence that the second co-IPd. This approach was used to assay for both hetero- and homodimer formation. Initial experiments with constructs containing only cytoplasmic RPTP domains showed no evidence for dimerization. A second round of experiments with full-length RPTPs yielded the same result. Relatively weak expression in the S2 cell culture system leaves open the possibility that negative results were due to an inability to detect low protein levels. More likely, formation of putative dimers depends on one or more co-factors not present in S2 cells.

MATERIALS AND METHODS

Plasmid Construction

Epitope-tagged constructs, denoted psmyc and psha, were manufactured using the S2 expression vector pRmHA3 as starting material. The PCRd cytoplasmic domain of each RPTP was subcloned into these base constructs. The salient features of the constructs include a metallothionein promoter for induction of expression with copper sulfate. A translation start consensus sequence is located immediately upstream of the initiator methionine for efficient expression. Immediately downstream of the initiator ATG, a Src myristylation sequence is present to direct the expressed protein to the inner surface of the cell membrane. The multiple cloning site includes five restriction sites selected to accommodate subcloning of RPTPs. Following the MCS is a single myc, ha or rho epitope tag, and finally a stop codon. 3' PCR primers were designed to ensure that the coding sequence of each RPTP domain is in frame with the epitope tag.

The finished constructs were sequenced by the Caltech Sequencing Facility to confirm accurate amplification of the RPTP cytoplasmic domains. Full-length, untagged versions of DPTP10D, DPTP69D and DPTP99A were made by fellow lab member Sarah Fashena by subcloning cDNAs into pRmHa3. The cytoplasmic (in psmyc) and full-length (in pRmHA3) DLAR constructs were made by Neil Krueger at Harvard University. Baculovirus constructs were made by cutting full-length RPTPs out of pRmHa3 and dropping them into the baculovirus vector pVL393.

DLAR mAb generation

A portion of the DLAR extracellular domain containing three FN III repeats was PCRd and subcloned into pVL393, a transfer vector containing a baculovirus promoter flanked by baculovirus DNA derived from the polyhedron gene. This was submitted to Peter Snow in the Protein Expression Facility, who manufactured the recombinant virus via homologous recombination. Dr. Snow purified the recombinant protein, which was then given to Susan Ou of the Monoclonal Antibody Facility. Monoclonal antibodies (mAbs) generated against the recombinant protein were initially screened with ELISA. Positive

clones were then tested for their ability to immunoprecipitate DLAR from cell lysates, and to recognize DLAR on Western blots. The mAbs 8C42F5 and 9D82B3 produced the best results and were used in combination for these experiments.

S2 cell transfection, induction, harvesting and lysis

Growth medium used for S2 cells consisted of Schneider's medium supplemented with 10% heat inactivated fetal calf serum, penicillin (100U/ml), streptomycin (100 μg/ml) and amphotericin B (0.25 μg/ml). 10^7 cells were plated on 10 cm tissue culture plates and expanded overnight (25º C, atmospheric pressure). Cells were transiently transfected with the DNA of interest (10 μg) using the calcium phosphate method. 18 hrs later the cells were washed with PBS and resuspended in growth medium. 0.3 mM $CuSO_4$ was added to induce the metallothionein promoter to drive expression. The cells were harvested 24 hrs later, washed in PBS and lysed in 450 μl of ice-cold lysis buffer (125 mM NaCl, 10 mM TrisCl pH 7.5, 0.2% Triton X-100, 600 μM PMSF, 2 mM Na_3VO_4, 25 mM NaF and 2 μg/ml APP). The lysate was spun briefly to pellet nuclei and insoluble membrane components.

Immunoprecipitations and Western blot analysis

Lysates were incubated with primary antibody and protein G+A agarose beads for 1 hr at room temperature. The agarose beads with bound immune complexes were spun down and washed with lysis buffer twice. The pellets were boiled for 3 minutes in SDS sample buffer. Samples were run on 9% polyacrylamide gels and transferred to a PVDF membrane. Blots were blocked in 5% dry milk in TBST (25 mM TrisCl pH 7.4, 137 mM NaCl, 0.2% Tween 20) for 30 minutes at RT. The blots were incubated in primary antibody for 1 hr, washed with TBST, and incubated with an alkaline phosphatase-conjugated goat anti-mouse secondary. After 30 minutes washing the blots were developed to detect phosphatase activity.

RESULTS

Cytoplasmic RPTP domains insufficient for dimerization

We tested for dimerization by transiently cotransfecting two RPTPs into S2 cells and inducing their expression. One RPTP was IPd, and if the other co-IPd it was taken as evidence in support of dimerization. Because it contains the active site and wedge domain, the RPTP cytoplasmic domain was considered sufficient to mediate the presumptive dimerization. By excluding the extracellular and transmembrane domains, the possibility of two RPTPs sticking together nonspecifically and being misinterpreted as a dimer is reduced. The cytoplasmic domain of each RPTP was PCRd and subcloned into an epitope-tagged S2 expression construct. A Src myristylation sequence was included in the construct to localize the expressed protein to the membrane. Other features of the construct are depicted in Figure 2.

S2 expression constructs made for each of three different epitope tags (myc, rho and ha) were tested with a uniform insert to determine which tag yielded the best immunoprecipitation results. The efficiency of IPs was roughly equivalent with the myc and rho epitopes, while the ha tag was considerably weaker. Unlike ha, myc and rho IPs were strong enough to provide results that could be interpreted reliably. RPTP cytoplasmic domains were subcloned into the myc- and rho-tagged expression constructs. Two constructs with dissimilar epitope tags were cotransfected in each experiment. Following a myc IP, the rho-tagged RPTP is visualized on a Western blot with an anti-rho antibody. The experiment is performed in a complementary manner as well, by IPing with a rho antibody and looking for evidence of the myc-tagged RPTP with an anti-myc antibody.

One difficulty encountered early in the course of experiments was variable expression of the transfected RPTP constructs. For reasons unknown, some constructs expressed well when transfected individually, but not when coexpressed with a second RPTP. Under these conditions the expression levels would drop off to varying degrees. The calcium phosphate method calls for 10 μg of the DNA being transfected, so in cotransfections 10 μg of each plasmid was used for a total of 20 μg. The two plasmids were introduced to the cells at the same time after mixing in a transfection solution.

Efficiency of transfection with calcium phosphate is roughly 10-20% for S2 cells. Certain measures were taken to increase the efficiency when dealing with a construct whose expression was inconsistent in cotransfections. This included increasing the amount of DNA (up to 20 μg), and lengthening the cell culture incubation time between addition of DNA and harvesting of cells.

Due to the variable expression of some constructs, it was important that our experimental design incorporate a positive control for protein expression. A result militating against dimerization is meaningful only when both RPTPs expressed well enough to be detected on a Western blot. It was also important to include a negative control to exclude antibody cross-reactivity as the reason for any observed co-IPs.

Results from a typical experiment are shown in Figure 3. In this experiment, two differently tagged versions of DLAR were cotransfected to look for evidence of DLAR homodimers. Two constructs expressing the DLAR cytoplasmic domain were transfected, one carrying a myc tag (DLARmyc) and the other a rho tag (DLARrho). Lysate from transfected cells was split in two; half was IPd with anti-myc and half with anti-rho. The myc IP was itself split in two, and the half probed with anti-myc shows a DLARmyc band, confirming expressed of DLARmyc. If DLARmyc complexed with any DLARrho, some of the latter should have come down with it. However, when the second half of this IP is probed with anti-rho, no DLARrho is visible. The negative result could be accounted for if DLARrho failed to express, since that would preclude a DLARrho/DLARmyc complex from forming. This possibility is eliminated when the second batch of lysate is IPd with anti-rho. The IP pellet is again split in two, and half is probed with anti-rho. The resulting DLARrho band confirms DLARrho did express. The other half of the pellet is probed with anti-myc. Despite the fact that DLARmyc and DLARrho were expressed alongside each other, the absence of a DLARmyc band here once again suggests that none of it formed a complex.

It is possible that our negative results are due to the fact that the cytoplasmic domain alone is insufficient to mediate dimerization. Perhaps the RPTP extracellular domain is necessary for the protein to assume the conformation required for forming dimers. This theory was tested by repeating the experiments, this time using constructs coding for full-length RPTPs.

No evidence for dimerization of full-length RPTPs

Subcloning of full-length RPTP coding sequences into the S2 cell expression vector pRmHa-3 had already been done for three of the RPTPs examined in this study. That left the full-length sequence of DLAR, which was cloned into the same vector by Neil Kreuger. Since the full-length constructs lack an epitope tag, antibodies were needed for each of the four RPTPs. mAbs against three of the four had previously been made in our lab. No antibody had been made against DLAR, so it was necessary to make one. We subcloned a portion of the DLAR extracellular domain including three FN III repeats into a baculovirus transfer vector. The vector was given to Peter Snow, who made the virus and expressed and purified the protein fragment. Susan Ou immunized mice with the polypeptide and performed the cell fusion. She supplied clones that were screened via ELISA. Finally, the strongest contenders were tested for their ability to IP DLAR. The resulting mouse mAb, 9D8, has proved efficient for IPs, Westerns and embryo staining.

The same experimental scheme used for cytoplasmic constructs (detailed above) was used with the full-length constructs. There was one procedural difference involving the method for Western blot development. The alkaline phosphatase method of detection that had been used previously was not sensitive enough for experiments with the full-length constructs. There appeared to be less protein on the blots, due to several possible causes. Perhaps the full-length constructs did not express as robustly as their cytoplasmic counterparts. The IPs may have been less efficient also; it may be more difficult to IP the larger full-length proteins (120-200 kD) than the smaller cytoplasmic versions (30-80 kD). Finally, this size discrepancy may also have been an issue in the transfer to the membrane (efficient transfer may be more difficult with larger proteins). In any case, switching to the more sensitive ECL detection method made the bands easier to visualize.

This round of experiments was no more successful than the first in yielding evidence for RPTP dimerization. As before, cotransfections with all possible pairwise combinations of RPTPs were performed to assay for both hetero- and homodimers. The results of a typical experiment are shown in Figure 4. S2 cells were cotransfected with full-length DLAR and DPTP99A. Half the cell lysate was IPd with anti-DLAR and half with anti-DPTP99A. The anti-DLAR IP pellet was split in two, and one half was probed with anti-DLAR. The resulting DLAR band confirms expression. The other half was

probed with anti-DPTP99A, and the absence of a band suggests no DPTP99A co-IPd. To verify that DPTP99A expressed, one half of the DPTP99A pellet was probed with anti-DPTP99A. The resulting band, so strong it appears as a large smear, confirms robust expression. Probing the second half of the pellet with anti-DLAR reveals that no DLAR co-IPd.

Results from experiments with DPTP10D may have been misinterpreted as evidence in support of dimers were it not for the negative control. The apparent co-IPs that were observed in cases where DPTP10D was cotransfected with other RPTPs turned out to be an artifact of DPTP10D's tendency to stick indiscriminately. In experiments where DPTP10D was cotransfected with a given RPTP "X," an IP with anti-X followed by an anti-DPTP10D blot would show a DPTP10D band. By itself, this suggests a DPTP10D/RPTP X dimer. The negative control was to IP a plate of cells transfected with only DPTP10D and IP with anti-X. If the dimer result is real, a DPTP10D band resulting from an anti-X IP should be seen only when X is coexpressed with DPTP10D. Because it appeared when DPTP10D was expressed alone, it must be attributable to cross-reactivity. We observed that in addition to mAbs against all RPTPs, protein G+A beads alone were able to precipitate DPTP10D. This suggests that instead of cross-reactivity, the results were caused by a nonspecific interaction of DPTP10D with the G+A beads.

DISCUSSION

Crystallographic data suggests RPTPs form dimers

The first evidence to suggest RPTPs form dimers similar to their RTK counterparts comes from crystallographic studies. In each of two independent crystal structures, murine RPTPα exists as a symmetrical homodimer, where the helix-turn-helix (or "wedge") domain of one RPTP inserts into the active site of its dimer partner (Bilwes et al., 1996). The active site of both RPTPs is sterically blocked due to this interaction, theoretically rendering the enzymes inactive. Indeed, RPTPα studies have documented an inhibition of phosphatase activity upon dimerization (Jiang et al., 1999). RPTPs have a conserved wedge domain upstream of the first catalytic domain, denoted D1, suggesting

that downregulation of catalytic activity via dimerization-induced active site occlusion may represent a paradigm for regulation of RPTPs in general.

Subsequent studies have shown that dimer interactions can be complex, with a domain from one RPTP inserting into the catalytic domain of a different RPTP to form cross-species heterodimers (Blanchetot and den Hertog, 2000; Gross et al., 2002). For example, the second catalytic domain (D2) of PTPδ has been shown to bind to D1 of RPTPσ, and this results in an approximately 50% reduction in the catalytic activity of the latter (Wallace et al., 1998). Evidence also exists for formation of multimers, where strings of RPTPs are interconnected via interactions between wedge and active site domains of neighboring molecules (Iversen et al., 2002).

Intramolecular interactions also exist, as in the case of RPTP LAR. Although direct evidence for a LAR homodimer is lacking, the crystal structure suggests D1 of one LAR molecule may interact with D2 of a second (Nam et al., 1999). However, any model of dimer mediated regulation presupposes that all RPTPs form dimers in which the active site is obstructed, and crystal structures of other RPTPs indicate at least some do not. For example, RPTPμ does exist as a dimer in the crystal structure, but the wedge domain of one subunit of the dimer is not inserted into the catalytic cleft of the dyad-related monomer. Consequently, the active site remains in an open, uninhibited conformation (Hoffmann et al., 1997). Activity regulation through dimerization may thus be a feature of only a subset of RPTPs, and a goal of future work will be to develop a more comprehensive account of which RPTPs belong in this category.

Evidence for in vivo dimer formation

Additional evidence for dimerization comes from recent cross-linking studies showing that RPTPα homodimerizes on the cell surface, suggesting that dimers form under normal physiological conditions (Jiang et al., 2000; Tertoolen et al., 2001). The same studies examined which of the RPTPα domains are necessary and/or sufficient for dimer formation. Remarkably, the results suggest no domain is absolutely required and that each is sufficient to mediate dimerization. Of all constructs tested, the ones where the wedge domain was included produced the most efficient dimer formation. Thus, although

multiple points of interaction are implicated in mediating dimerization of RPTPα, the wedge domain appears to play the major role.

Homodimers still form when the wedge domain is eliminated, albeit with the efficiency of dimerization significantly reduced. Thus, the region implicated by crystallographic studies as the major mediator of dimerization appears upon closer inspection to be important but not essential. Homodimers still form when the extracellular domain (ECD) is missing, so it too is not essential for dimerization. However, it is sufficient for homodimerization, as determined with a fusion protein comprised of the ECD with a C-terminally fused GPI-linker for membrane insertion. Finally, even the transmembrane domain when expressed by itself forms a homodimer. The net result of these experiments suggests a "zipper" model wherein multiple interactions occur along length of the RPTP, each contributing to formation of a stable dimer.

Several lines of evidence support model of dimer mediated negative regulation of RTPT activity

Regulation of catalytic activity is well understood for the counterparts to the RPTPs, namely the RTKs. Following addition of ligand, RTKs dimerize and autophosphorylate, thereby switching on activity. A growing body of evidence suggests that RPTPs may work in the opposite manner, with dimerization inhibiting instead of promoting biological activity. Experiments with an EGF/CD45 chimera were the first to suggest this alternate theory of regulation. CD45 is an RPTP with no known ligand that is expressed on all nucleated hematopoietic cells and is required for TCR signaling in response to engagement of antigen receptor. To study the effects of dimerization on CD45 activity, a chimeric protein was made with the extracellular and transmembrane domain of EGF fused to the intracellular domain of CD45. Addition of EGF to cells expressing the chimera results in a loss of TCR signaling, suggesting that induced dimerization extinguishes the catalytic activity of CD45 (Desai et al., 1993; Majeti et al., 1998).

The EGF/CD45 chimera data is consistent with results from another study involving induced dimerization. In this case, a point mutation in the extracellular domain of full-length RPTPα causes constitutive homodimerization via a disulfide bond. The FL-137C

mutant was transfected into fibroblasts from RPTPα knock-out mice to assay its ability to dephosphorylate (and thereby activate) its c-Src substrate. Results indicate the mutant activates c-Src significantly more weakly than WT RPTPα. Additional point mutations in the wedge region of FL-137C restore c-Src activation to a level comparable to that of WT. Separately, the dimerization efficiency of RPTPα with the same wedge domain point mutations is shown to be significantly lower compared to WT RPTPα (Jiang et al., 1999).

In addition to biochemical evidence for a physiological role for dimerization, genetic data from our lab can be interpreted in a manner consistent with the dimer model. RPTP DLAR is required for proper execution of several discrete axon guidance events during *Drosophila* nervous system development. One example is entry of the intersegmental nerve b (ISNb) into the ventrolateral muscle field (VLM) after defasciculation from the intersegmental nerve (ISN). In embryos with a DLAR null mutation, the ISNb fails to enter the VLM approximately 25% of the time. However, in embryos that are doubly mutant for both DLAR and DPTP99A, this guidance error is reduced to about 2% (Desai et al., 1997). Other guidance mistakes observed in DLAR null mutants are not affected by removal of DPTP99A, suggesting a specificity in the suppression of this phenotype. This result implies that in the DLAR mutant, ISNb continues along its original trajectory instead of turning into the VLM because of inappropriate DPTP99A activity. Thus, the function of DLAR at this choice point is to counteract or suppress DPTP99A signaling. One way it could do that is by forming a heterodimer that, like other dimers studied, is catalytically inactive.

Taken together, these results support a theory of dimer mediated negative regulation of RPTP activity. In this model, RPTP activity would be switched on by ligands that dissociate dimers, or by intracellular processes such as phosphorylation that would transform the intracellular domains of existing dimers into an open conformation.

No evidence for stable dimer formation in S2 cells

Despite strong evidence that dimerization is a common means by which RPTP activity is modulated, we were unable to find any evidence for stable dimer formation under the conditions tested. If the RPTPs we studied are induced to dimerize by binding of ligands,

one possibility for these negative results is that these ligands are not expressed in S2 cells. There are currently no known ligands for the four RPTPs examined in this study, so we were unable to assess whether ligand binding induces dimerization. A secreted factor has been identified that interacts with and inhibits the activity of RPTPβ (Meng et al., 2000), so it is reasonable to assume that ligands for other RPTPs do exist. The RPTPs' large extracellular domains resemble those of cell adhesion molecules and have a high degree of variability, consistent with their having unique ligand binding specificities. Once a ligand for these RPTPs is identified and cloned, it can be added to the cell culture system to determine whether it facilitates dimer formation.

It is also possible that only a small fraction of the transiently expressed full-length RPTP makes it to the cell surface in our experiments. If most of the expressed protein is located intracellularly, it may be unable to assume the conformation necessary for engaging in dimer interactions.

Finally, our experimental conditions may permit transient dimer formation, but may not be conducive to formation of dimers stable enough to remain intact during the immunoprecipitation process. It is also possible that a small fraction of dimers do remain intact but are below the limits of detection.

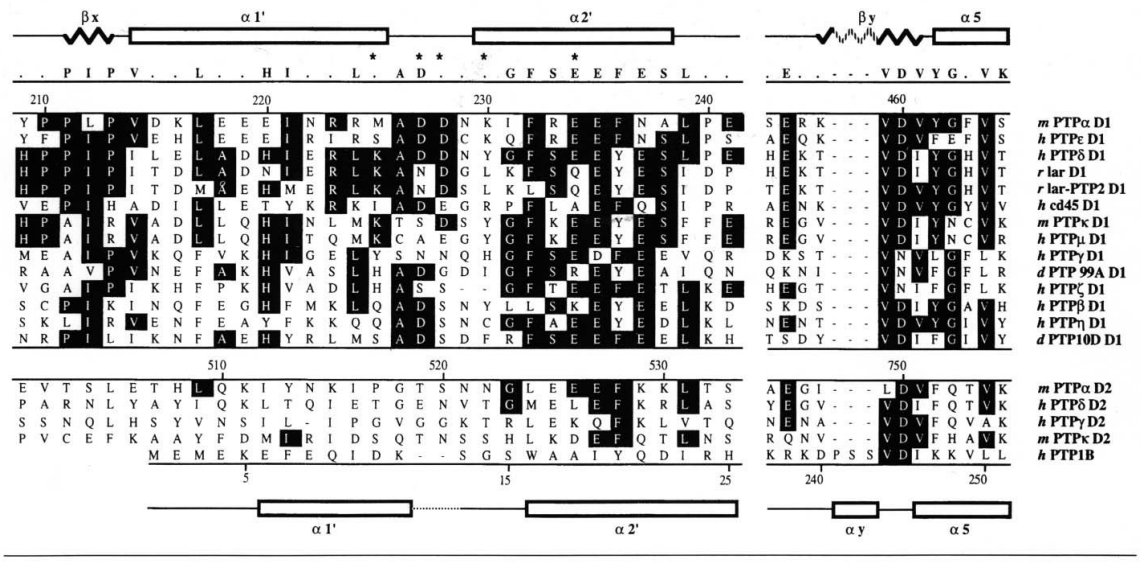

Figure 1. Sequence alignment of the N-terminal wedge of RPTPs' membrane-proximal catalytic domains. Line one schematically illustrates the secondary structural elements observed in RPTPαD1. Line two gives the consensus sequence conserved across the large family of D1 domains. The numbering scheme refers to the short variant of murine RPTPα with the first residue of the signal peptide numbered as 1. The stars indicate residues involved in active-site-directed dimeric interactions. Residues boxed in black are common to at least five aligned sequences. (*m* is mouse, *h* is human, *r* is rat, and *d* is *Drosophila*). The first 14 homologous sequences contrast sharply with the lack of sequence conservation in the final segments. The most distinguishing feature of the RPTP N-terminal wedge involves a two-amino-acid insertion (Asp 227 and Asp 228) into the tip of the non-receptor-like PTP N-terminal segment. The second to the last line corresponds to the numbering scheme of human PTP1B. The final line emphasizes the structural elements observed in the PTP1B crystal structure.

Source: Nature (1996) **382**, 559

Figure 2. psmyc schematic

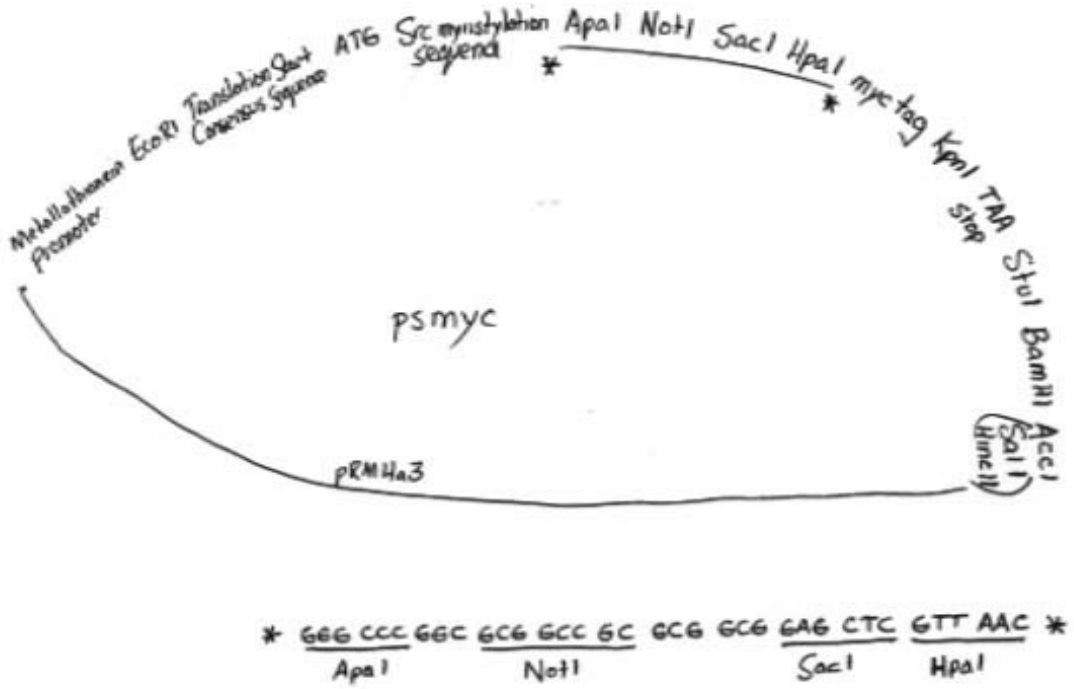

Figure 3. DLAR homodimer experiment

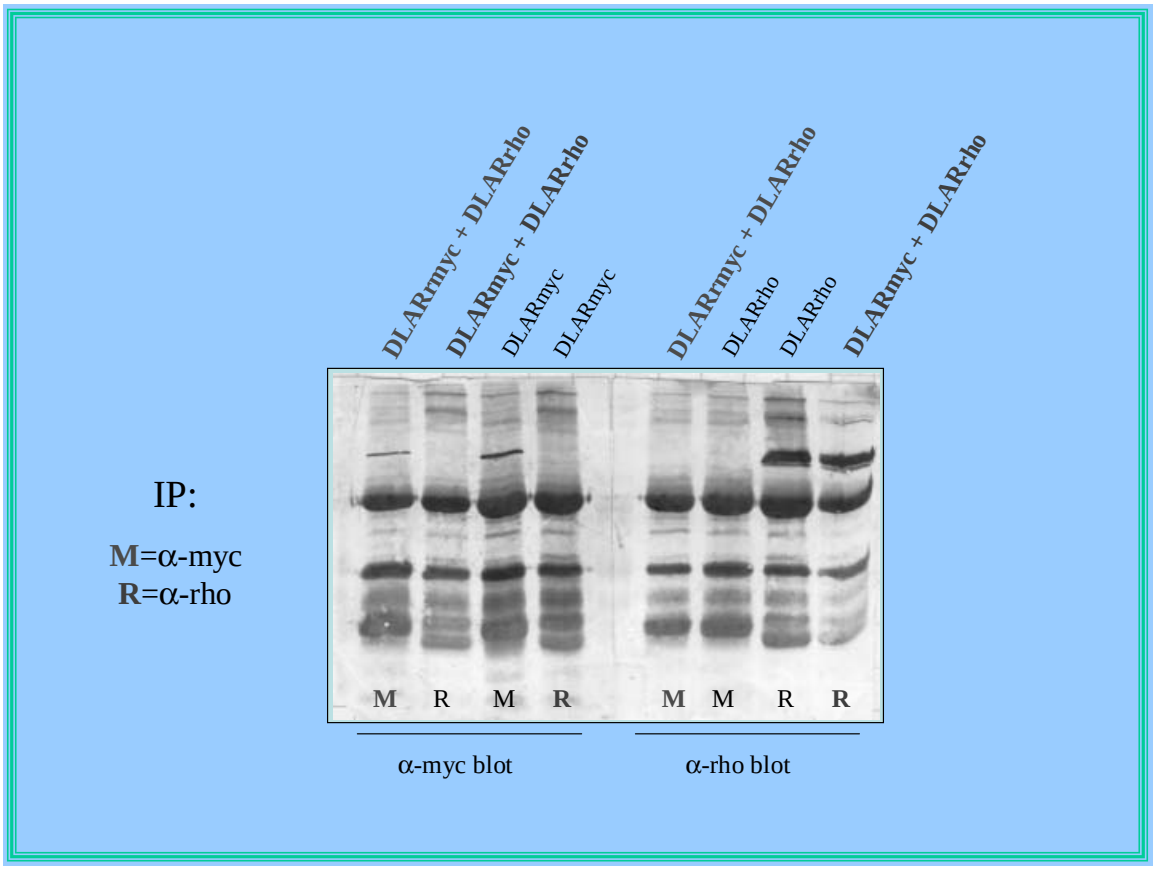

Figure 4. DLAR/DPTP99A heterodimer experiment

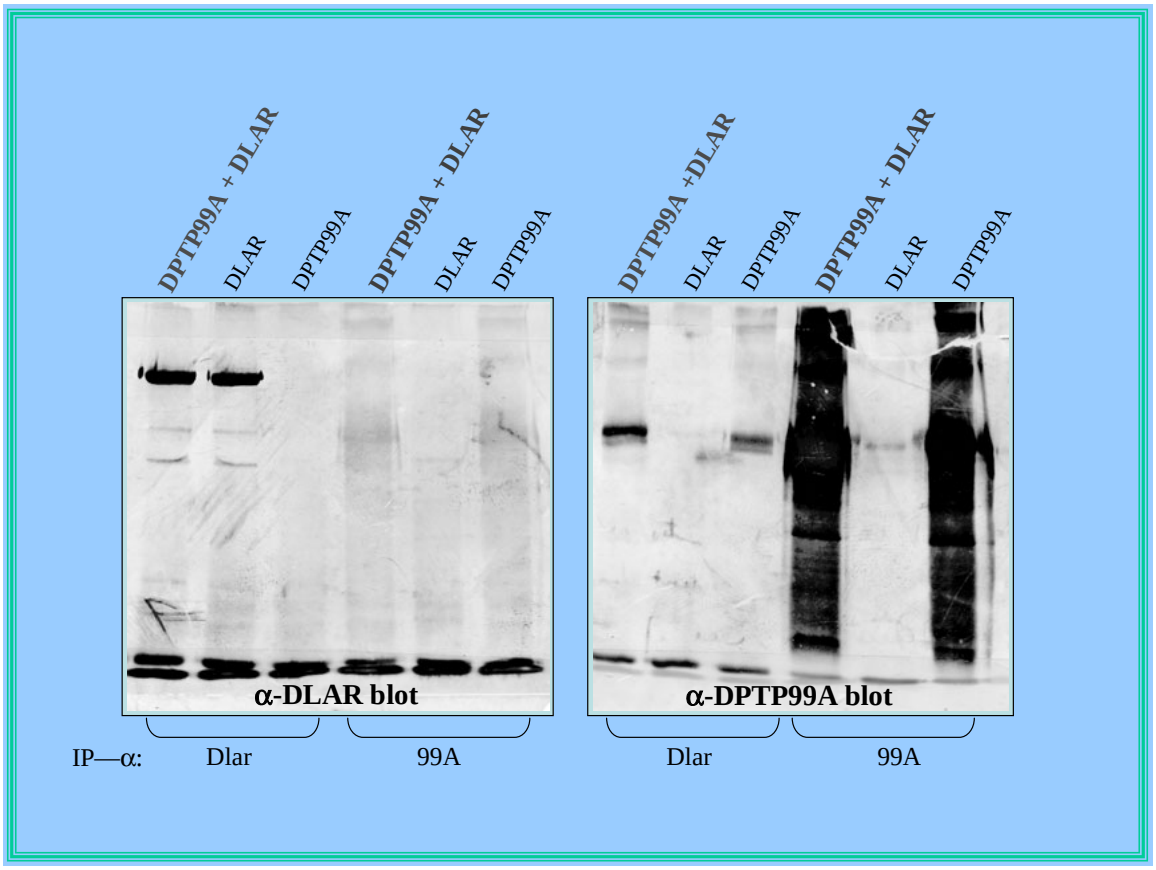

Table 1. S2 cell transfection experiments

Heterodimer experiments	Homodimer experiments
DPTP69D FL + DPTP10D cyto myc	DPTP69D FL + DPTP69D cyto myc
DPTP69D FL + DLAR FL myc	DPTP99A FL + DPTP99A cyto myc
DPTP69D FL + DLAR cyto myc	DPTP10D FL + DPTP10D cyto myc
DPTP69D FL + DPTP99A FL	DLAR FL + DLAR cyto myc
DPTP69D FL + DPTP10D FL	DLAR cyto rho + DLAR cyto myc
DPTP99A FL + DPTP69D cyto myc	
DPTP99A FL + DLAR FL myc	
DPTP99A FL + DLAR cyto myc	
DPTP10D FL + DLAR cyto myc	
cyto=cytoplasmic domain, FL=full-length	

Chapter 3

Biochemical analysis of potential interactions between RPTPs and Robo receptors

Abstract

Robo is the guidance receptor for the *Drosophila* midline repellent Slit. Robo signaling is required to keep axons from inappropriately crossing the midline. Robo and receptor-linked tyrosine phosphatases (RPTPs) are expressed in growth cones during axonogenesis and several genetic observations suggest that Robo signaling involves the activity of RPTPs DPTP10D and/or DPTP69D. We show here that Robo is phosphorylated on one or more tyrosine residues, a feature characteristic of phosphatase substrates. No evidence was seen, however, for a biochemical interaction between Robos and “substrate trap” versions of the RPTPs, leaving us to conclude that RPTPs’ contribution to Robo signaling may be downstream of Robo.

INTRODUCTION

Many extracellular signals, once transduced to the cell interior, are ultimately manifest as a change in the tyrosine phosphorylation status of specific regulatory proteins. Two classes of enzymes, protein tyrosine kinases (PTKs) and protein tyrosine phosphatases (PTPs), work coordinately to regulate intracellular phosphotyrosine levels. Together they are involved in a diverse number of cellular processes including differentiation, proliferation and axon guidance. PTPs can be divided into two classes: receptor-like PTPs that span a membrane, and cytoplasmic PTPs. The receptor PTPs (RPTPs) have extracellular domains comprised of N-terminal immunoglobulin (Ig) domains and membrane-proximal fibronectin type III (FNIII) repeats. The structure of their ectodomain is thus similar to that of cell adhesion molecules, implicating them in participating in cell-cell, cell-extracellular matrix adhesive events underlying axon pathfinding. The intracellular domain of most RPTPs is comprised of two protein tyrosine phosphatase catalytic domains denoted D1 and D2. The membrane-proximal D1 domain has most or all of the catalytic activity, while the C-terminal D2 has little or none. The high degree of sequence conservation in D2 among members of the RPTP family suggests it may have an indispensable function unrelated to catalysis. Among the proposed roles for D2 are binding of substrates and/or downstream regulatory factors. This domain may also regulate activity by inserting into the active site of dimerized RPTPs, thereby precluding substrates from binding. Recent findings that RPTPα homodimerizes in vivo are consistent with this model (Tertoolen et al., 2001), yet we have found no evidence for dimerization in the RPTPs controlling axon guidance in *Drosophila* (see Chapter 2).

The role of RPTPs in axon guidance and synaptogenesis has been studied extensively in *Drosophila*. During axonogenesis, four RPTPs (DPTP69D, DPTP99A, DPTP10D and DLAR) are selectively expressed on CNS axons and growth cones (Tian et al., 1991). They interact with each other in various well-defined ways to facilitate a given axon's navigation from one choice point to the next en route to a final target destination. In some cases they work antagonistically, while in others they collaborate to regulate guidance decisions (Desai et al., 1997; Sun et al., 2001). Mutations in these

enzymes result in characteristic axon guidance phenotypes. However, a mutation in any single *Rptp* gene usually has no effect on guidance decisions. Most axon guidance phenotypes are observed only under conditions where two or more *Rptps* are mutant. This suggests partial redundancy in the function of these genes.

Ptp69D and *Ptp10D* provide one example of the redundant nature of the *Rptp* genes. When either gene is mutated individually, no phenotype is observed and embryos are both viable and fertile. However, in embryos doubly mutant for both *Ptp69D* and *Ptp10D*, a strong phenotype in the ventral nerve cord is observed. The nerve cord is the fly equivalent of the vertebrate spinal cord and is comprised of a ladder-like scaffold of axons. The upright parts of the ladder are formed by longitudinal axon bundles called connectives, while the rungs are formed by segmentally reiterated pairs of bundles called commissures. The decision to cross the nerve cord midline underlies the formation of these two bundle types: axons that choose to remain on one side of the midline form longitudinals, while those that make the decision to cross form commissures. In the *Ptp69D Ptp10D* double mutant, axons that normally do not cross the midline follow abnormal midline-crossing pathways, resulting in a highly disorganized nerve cord (Sun et al., 2000).

The *Ptp69D Ptp10D* double mutant phenotype resembles that of embryos mutant for Roundabout (Robo). Robo is the receptor for a protein called Slit, which is secreted by midline glial cells (Brose et al., 1999). Slit, a midline repellent, mediates the repulsion of Robo-expressing growth cones (Kidd et al., 1999). Robo is expressed in all nerve cord axons, so how is it that some are able to cross the midline? The answer has to do with a third protein called Commissureless (Comm) which is expressed in commissural axons and midline glial cells. Recent findings show that the function of Comm is to sort Robo to endosomes, where it is degraded (Keleman et al., 2002; Myat et al., 2002). As a result of this sorting function, no Robo makes it to the cell surface in Comm-expressing axons. This makes them impervious to the repellent qualities of Slit, enabling them to cross the midline. Comm expression ceases after the axons have crossed, and the axons are once again sensitive to Slit due to Robo on their cell surface. This keeps them from inappropriately recrossing the midline.

Several lines of genetic evidence show that DPTP69D and/or DPTP10D may be positive regulators of Robo signaling (Sun et al., 2000). First, a *Ptp69D Ptp10D* double mutant has a midline crossing phenotype that resembles that of a *robo* mutant in some respects. Second, the same double mutation partially suppresses the phenotype of *comm* mutants. In *comm*- embryos, all Robo localizes to the cell surface because there is no Comm sorting it to endosomes. Consequently, all axons are sensitive to Slit and repelled from the midline. Introduction of the *Rptp* double mutant into this background results in some axons crossing the midline, suggesting that Robo's signaling has been compromised. In the third line of evidence, the double mutant is introduced into a *slit*- background. When one copy of *slit* is removed, enough repulsive signaling remains to keep axons from crossing the midline inappropriately. That is no longer true when *Rptps* are removed as well, and less efficient Robo signaling is a plausible interpretation.

No substrates have yet been identified for the RPTPs, but the above genetic data led us to speculate that Robo may be a substrate for DPTP69D and/or DPTP10D. Consistent with this, Robo has an intracellular phosphotyrosine consensus motif. If this prediction is correct, robust signaling through Robo may require not only Slit binding but also dephosphorylation by an RPTP. Lending credence to this theory, Robo appears to be negatively regulated by Abl tyrosine kinase signaling, and a Y-to-F mutation in this motif produces a gain-of-function phenotype (Bashaw et al., 2001). Additional features of Robo that make it suitable for consideration as an RPTP substrate include its being expressed at the same time (axonogenesis) and in the same place (growth cones) as RPTPs. Furthermore, as a surface protein it has the same subcellular localization as RPTPs.

A prerequisite for any RPTP substrate is that it is tyrosine phosphorylated. We show here that Robo1 and Robo2 are phosphorylated by the tyrosine kinases Src and Abl. This finding encouraged us to pursue experiments to test whether Robos are RPTP substrates. We cotransfected S2 cells with Robo and a substrate trap version of DPTP10D (DPTP10D trap) or DPTP69D (DA3). The substrate traps have a point mutation that causes them to remain bound to substrate (Flint et al., 1997). In some cases trap proteins are rendered useless because phosphorylation on certain residues sterically hinders the binding of substrate. Our results show that RPTP traps used in this study are not phosphorylated, and thus not precluded from binding substrate. In spite of this, and

contrary to data favoring an enzyme/substrate relationship, our results show no evidence that Robo is a substrate for RPTPs. It is possible this is due to a requisite co-factor being absent from the cell culture system. However, it is equally plausible that RPTPs contribute to Robo signaling by dephosphorylating other proteins in the Robo pathway.

RESULTS

The approach we took to determine whether Robo is an RPTP substrate was as follows. First, ascertain whether Robos are phosphorylated on tyrosine residues. If they are, they meet a basic prerequisite for potential RPTP substrates. Provided this result is positive, cotransfect Robo and RPTP substrate trap constructs, immunoprecipitate the mutant RPTPs and look for Robo. If Robo co-IPs, it suggests there is an interaction between the proteins. That would be the basis for proceeding with the next set of experiments, designed to determine the particular type of interaction. Specifically, we are interested in looking for evidence of an enzyme-substrate interaction. This involves two separate cotransfections, one with wild type RPTP and Robo, the other with substrate trap RPTP and Robo. Once again, the RPTPs are immunoprecipitated and the associated Robo is visualized on a Western blot. If the amount of Robo that co-IPs with the RPTP trap is significantly greater than what copurifies with WT RPTP, this would be evidence in support of the enzyme-substrate interaction. However, if the amount of copurifying Robo is the same in both cases, it would suggest a different type of interaction.

As experiments testing for Robo phosphorylation began, the RPTP trap plasmids were constructed. The nature of the trap mutation can be understood in the context of the dephosphorylation reaction. All phosphatases have a conserved catalytic domain of approximately 240 residues that is characterized by a signature motif: (I/V)HCXAGXXR(S/T)G. This motif contains an invariant cysteine residue that is essential for catalytic activity. It acts as a nucleophile and attacks a phosphorus-oxygen bond in the substrate, leading to formation of a thiol-phosphate intermediate. Binding of substrate induces a conformational change in the enzyme, causing movement of a loop that forms one side of the active site cleft. This results in a more closed structure around

the active site and brings the side chain of an invariant, catalytically essential aspartic acid into position to act as a general acid. The aspartic acid has an abnormal pK value, so that it is protonated, and can donate the proton to the oxygen of the phosphorylated tyrosine residue, making the bond of the phosphorus to this oxygen more labile. This facilitates nucleophilic attack by the cysteine residue and thus allows dephosphorylation to occur (Zhang et al., 1994b).

The mutation that turns an RPTP into a trap is a single point mutation in the invariant aspartic acid. If this residue is replaced by one that cannot act as a proton donor, the phosphate-tyrosine bond cannot be efficiently hydrolyzed and the enzyme-substrate complex is stabilized enough such that it can be isolated. This approach has been used successfully in many cases, leading to the identification of a number of substrates for a variety of RPTPs. For example, the EGF receptor was identified as a PTP1B substrate and $p130^{cas}$ was identified as a substrate for PTP-PEST (Flint et al., 1997; Garton et al., 1996).

Robo1 and Robo2 are phosphorylated in vitro by *Drosophila* tyrosine kinases

Phosphorylation on one or more tyrosine residues is the sina qua non of a tyrosine phosphatase substrate. Robo has a phosphotyrosine consensus domain, but whether it was actually phosphorylated was unknown. To determine whether Robo met this minimum requirement for consideration as an RPTP substrate, we transfected S2 cells with Robo and one of two *Drosophila* tyrosine kinases. All of the Robo constructs and Robo mAbs used in this study were provided by the Goodman lab at UC Berkeley.

Three plates of S2 cells were transfected, one with Robo1 and Src kinase, one with Robo1 and Abl kinase, and one with Robo1 alone. A Robo1 antibody was used to IP, and the resulting IP pellets were split across two lanes. One set of lanes was probed with anti-Robo mAb to control for the amount of Robo expressed, and the other set was probed with an anti-phosphotyrosine mAb. The Robo blot indicates an equivalent amount of Robo1 was expressed in each plate. The phosphotyrosine blot shows a band that co-migrates with Robo1 and is significantly stronger in the lanes corresponding to plates transfected with both Robo1 and a kinase (Figure 2). If Robo1 were not capable of being phosphorylated, the amount of phosphorylated Robo1 detected would be the same

regardless of whether a kinase was included in the transfection. Since addition of kinase does result in an increase in phosphorylated Robo1, it proves this protein is phosphorylated.

The same experiment was performed with Robo2, only in this case the myc antibody was used to IP as the Robo2 construct includes a C-terminus myc tag. Once again, Robo2 expressed at the same level in all three plates, but the ones in which kinase was cotransfected had noticeable higher levels of phosphorylated Robo2 (Figure 2). These results establish that the consensus domain for phosphorylation in Robo1 and Robo2 is used, making them potential RPTP substrates.

Substrate trap RPTPs show little or no tyrosine phosphorylation

Although the substrate trap approach to RPTP substrate identification has proved effective, a sizable number of cases exist where trap proteins have failed to identify substrates. One of the reasons traps may not work as expected has been elucidated by the Tonks lab. They found that some RPTPs trap mutants become tyrosine-phosphorylated on another residue via transfer of phosphate from substrates. This new phosphotyrosine then interacts with the active site cleft of the trap in an intramolecular interaction, resulting in occlusion of the trap. As a result, some RPTP traps do not efficiently form complexes with substrates.

To determine whether our RPTP traps were susceptible to inactivation via phosphorylation, we cotransfected myc-tagged cytoplasmic versions of the traps with both Src and Abl tyrosine kinases. Following a myc IP, the pellet was split across two lanes of an SDS-PAGE gel. After electrophoresis and transfer to a membrane, one set of lanes was probed with an anti-myc mAb to confirm expression of the RPTP trap. The second set of lanes was probed with an anti-phosphotyrosine mAb to detect the amount of phosphorylated RPTP trap. The myc blot show that DPTP10D trap expressed robustly, while the corresponding lane in the phosphotyrosine (pY) blot shows that none of it was phosphorylated. In the case of DPTP99A trap, a band can be seen in the pY blot that comigrates with the DPTP99A trap band in the myc blot, suggesting that some of the trap is phosphorylated. However, the intensity of the pY band is very weak relative to that of the myc band, so the fraction of trap protein that is phosphorylated is likely quite small.

Furthermore, the pY band resulting from cotransfection of DPTP99A trap with Src and Abl is no stronger in its intensity than the pY band resulting from transfection of DPTP99A trap alone. In light of this evidence showing the kinases cannot phosphorylate DPTP99A trap, it is likely that the bands in the pY blot reflect nothing more than a low level of background phosphorylation (Figure 3).

Robos are not trapped by RPTP trap proteins

To test for an interaction between Robo and RPTP trap proteins, we cotransfected them into S2 cells in various pairwise combinations. We IPd one and looked for evidence of the other using the appropriate controls: positive for protein expression and negative for antibody cross-reactivity. Src or Abl tyrosine kinase was included in every transfection. If Robo is an RPTP substrate it would need to be in its phosphorylated form to bind to the trap, and these kinases were shown to phosphorylate Robo in earlier experiments (see above). We conducted three sets of experiments, one for each Robo protein (Robo1, Robo2 and Robo3). While the experimental design was the same in each set of experiments, some parameters were altered in order to suit differences in the Robo constructs' epitope tag, promoter element or expression level (see below).

In the case of Robo1, initial experiments were hampered by low expression of the Robo1 construct. To overcome this problem we switched to a line of cells stably expressing Robo1. The high levels of endogenously expressed Robo1 in this line obviated the need for transfecting Robo1. Accordingly, DA3 (DPTP69D trap) and DPTP10D trap were transfected along with Abl into these cells. The experiment was performed in a complementary manner: one plate was IPd with anti-DPTP69D or anti-DPTP10D to see if Robo1 co-IPd, while a second plate was IPd with anti-Robo to see if DA3 or DPTP10D trap co-IPd. Protein expression was adequate as indicated by the positive control lanes. However, the experimental lanes show no evidence that Robo1 interacts with full-length trap versions of either DPTP69D or DPTP10D. Note that a DPTP10D trap band is visible on the anti-DPTP10D blot in the lane corresponding to the Robo1 IP. This suggests DPTP10D trap copurifies with Robo1, but this result is not corroborated when the experiment is done in the opposite direction (i.e., no Robo1 band is visible on the anti-Robo blot in the lane corresponding to the anti-DPTP10D trap IP).

We therefore conclude the result is an artifact attributable to the documented tendency of DPTP10D to stick indiscriminately (Figure 4).

Testing for Robo2 interactions with DA3 and DPTP10D trap was done in an analogous manner, only in this case a stable Robo2 cell line was used. Src was substituted for Abl, but this change should have no material effect since both kinases phosphorylate Robo2 equally well. The data indicate Robo2 does not interact with the RPTPs. The Robo2 blot was overdeveloped in an effort to bring out the bands corresponding to the RPTP trap IPs, but no trace of Robo2 is visible (Figure 5).

A stable Robo3 cell line was not available for the third set of experiments, so normal S2 cells were used instead. The Robo3 construct has a UAS promoter, so a GAL4 plasmid was required to drive expression. The constituent components of the transfection included UAS-Robo3, metallothionein-GAL4, Abl, and UAS-DA3. The metallothionein construct was induced with copper sulfate to express GAL4, which in turn drove expression of Robo3 and DA3. Positive controls show strong Robo3 expression as well as high levels of DA3. The experimental lanes are devoid of bands that would supply evidence for an interaction between these two proteins (Figure 6).

RPTP/Robo/Slit protein complex is not observed in S2 cells

When our biochemical experiments failed to show signs of an interaction that was predicted by a strong body of genetic evidence, we speculated that Robo may require the presence of its ligand, Slit, in order to interact with RPTPs. We tested this possibility by performing cotransfections in a stable Slit cell line. DA3 was cotransfected with Robo1 and Robo2 in separate experiments. In neither case did the presence of Slit facilitate an interaction. Results were the same as those from experiments where Slit was not included. We conclude that formation of the putative complex may require one or more additional co-factors not expressed in S2 cells.

DISCUSSION

RPTPs have a multifaceted role in developing organisms, important for a variety of developmental processes including cell differentiation and proliferation. In the case of axon guidance, RPTPs are thought to transduce cues in the local environment traversed by the growth cone into changes in intracellular phosphotyrosine levels, inducing a cascade of signaling that ultimately results in restructuring of the growth cone cytoskeleton. This allows the growth cone to change direction and reorient itself towards its target. The four Rptps expressed selectively in *Drosophila* CNS growth cones during axonogenesis (DPTP69D, DPTP99A, DPTP10D and DLAR) work collaboratively and competitively to assist axons in making correct guidance decisions. Mutations in these *Rptps* are associated with characteristic guidance defects. One area where defects caused by *Rptp* mutations have been studied extensively is the embryonic nerve cord.

The equivalent of the CNS in vertebrates, the nerve cord is a ladder-like structure located ventrally in flies. Proper wiring of the nerve cord involves the action of two opposing forces. Attraction to the nerve cord midline is mediated by *netrin* and *frazzeled* (Kolodziej et al., 1996; Mitchell et al., 1996), while repulsion away from the midline is mediated by *slit* and *robo* (Brose et al., 1999; Kidd et al., 1999). When repulsive signaling wins out, axons follow an ipsilateral pathway and form the nerve cord longitudinals. Conversely, when attraction wins axons cross the midline to form the two segmentally repeated commissures.

In commissural axons, repulsive signaling must be established once axons have crossed the midline to prevent them from recrossing. The key to this is a protein called Commissureless (Comm). Recent evidence has shown that Comm's main function lies in the sorting of Robo (Keleman et al., 2002; Myat et al., 2002). Commissural axons are able to cross the midline because Comm sorts all Robo synthesized by the cell to endosomes, where it is subsequently degraded. With no Robo reaching the cell surface, there is no opportunity for it to bind Slit and initiate repulsive signaling. After the axon has crossed the midline, Comm expression is downregulated and Robo reaches the cell surface instead of being sorted to endosomes. The repulsive signaling that ensues prevents axons from recrossing the midline.

With the details of this system worked out it is now possible to clearly interpret phenotypes that result when one of the component proteins, such as Robo, is mutated. In *robo* mutants, the receptor mediating repulsive signaling is absent so axons repeatedly cross the midline. The resulting axonal loops around the midline give it the appearance of the sort of roadway roundabouts common in European countries.

A different phenotype is observed when *slit* is mutated (Rothberg et al., 1990). Slit is secreted by midline glial cells and repels Robo-expressing growth cones. When *slit* is mutated, there is no repulsive signaling through any of the Robo proteins. The attractive signal mediated by Netrin and Frazzeled thus goes unopposed, and all axons are pulled towards and remain at the midline, resulting in a slit-like structure. *robo*- and *slit*-phenotypes differ because Robo is actually a family of three related proteins. When one Robo is mutant, the presence of the other two means that some repulsive signaling remains. However, when *slit* is mutated all Robos are effectively silenced and repulsive signaling is entirely eliminated.

Mutated *comm* causes yet another midline phenotype (Seeger et al., 1993). When Comm is absent no Robo is sorted to the endosomes and it all makes it to the cell surface. There it is free to bind Slit and mediate a constitutive repulsive signal, keeping all axons away from the midline. The result is a nerve cord lacking commissures, hence the name of the phenotype, “commissureless.”

Genetic data suggests RPTPs participate in Slit/Robo signaling

In addition to *robo*, *slit* and *comm*, mutations in *Rptps* have been found to produce midline phenotypes (Sun et al., 2000). Genetic experiments in which RPTP activity is ablated suggest the activity of these enzymes is required for the repulsive signaling mediated by Slit/Robo. For example, in the *Ptp69D Ptp10D* double mutant, axons cross the midline repeatedly to produce a looping phenotype that closely resembles *robo*-.

A PTP mutation in a *comm*- background is another case suggesting RPTP activity is a positive regulator of the Slit/Robo signaling pathway. In *comm* mutants, constitutive repulsive signaling prevents axons from crossing the midline to form commissures. When an *Rptp* mutation is introduced into this background some commissural axons do cross the midline, suggesting Slit/Robo signaling has been compromised.

In a *slit*- background, an *Rptp* mutation provides further evidence of a shared signaling pathway. Embryos heterozygous for *slit* should have less repulsive signaling due to diminished expression of this Robo ligand. The fact that no phenotype is seen suggests enough repulsive signaling remains for the embryo to develop normally. When combined with an *Rptp* mutation that is no longer the case, as axons are observed to cross the midline excessively.

Robo meets criteria for being an RPTP substrate

Although the importance of RPTPs in axon guidance is supported by a large body of evidence, little is known about the ligands and substrates for this integral class of proteins. The above genetic evidence supports the hypothesis that Robo may be an RPTP substrate. Several other features of Robo are consistent with this possibility. For example, it is expressed at the same time and place as RPTPs, namely during axonogenesis in motoneuron growth cones. Also, we show here that Robo is capable of being tyrosine phosphorylated, meeting the most fundamental requirement for consideration as a potential RPTP substrate.

The genetic data described above suggests that RPTPs interact with a repulsive signaling pathway mediated by Robo, Comm and Slit. In this protein trio, only Robo has the right subcellular localization to be considered an RPTP substrate. New evidence shows Comm is active intracellularly, sorting Robo to endosomes for degradation when the axon crosses the midline. Before and after crossing, Robo is at the cell surface where it would be able to interact with other cell surface proteins such as the RPTPs.

RPTP trap data does not support RPTP/Robo enzyme/substrate model

One way to interpret the above genetic data is to speculate that Robo activation requires not only Slit binding, but also dephosphorylation by RPTPs. To test whether Robos are in fact RPTP substrates, we used trap versions of the RPTPs to exploit their tendency to remain associated with a substrate once it has bound. Some traps are vulnerable to tyrosine phosphorylation on certain residues that precludes them from binding substrate. Our results suggest this issue does not apply to the RPTPs used in this study. In spite of

this, and separate experiments showing Robos are phosphorylated, the results of our cotransfection experiments testing for an RPTP/Robo interaction were negative.

Three Robo proteins are expressed in the CNS and we tested all three for their ability to bind substrate trap versions of DPTP69D and DPTP10D. Several approaches were taken to acquire evidence for such an interaction. In most cases, the Robos were cotransfected with a myc-tagged RPTP trap. Normal S2 cells were used for the initial experiments, but poor Robo expression made it difficult to clearly interpret results. Switching to a stable Robo-expressing line boosted the Robo signal enough to overcome this problem. When results from these experiments were negative we switched to a stable Slit-expressing cell line for cotransfections. The presence of the Robo ligand did not facilitate formation of an RPTP/Robo complex. A table showing all permutations of the experiments is shown in Figure 6.

RPTPs' contribution to Slit/Robo signaling pathway may lie downstream

Several reasons could explain the lack of evidence for an RPTP/Robo interaction. One is that RPTPs and Robo interact as part of a large protein complex. Formation of the complex may depend on the presence of each of its constituent members, some of which may not be expressed in S2 cells. We speculated that such a complex may be comprised of Robo, Slit and both RPTPs. To test this theory we cotransfected both RPTP traps into stable Robo cells and induced their expression with media from Slit cells. No evidence of complex formation was observed, suggesting additional proteins contribute to the putative complex. The "missing link" may be discovered upon further elucidation of the Robo/Slit signaling pathway.

A different interpretation of the role of RPTPs in Robo signaling could also account for our negative results. A preponderance of evidence, genetic and otherwise, suggests DPTP69D and DPTP10D participate in a signaling pathway mediated by the Robo receptor. Since Robo is capable of being phosphorylated, it is natural to assume that the RPTPs' role in this pathway is to dephosphorylate Robo, but it may be that one or more Robo effectors are the target(s) of the RPTPs. Since nothing is known about the signaling pathway downstream of Robo, there may exist several effectors that must be

dephosphorylated for efficient transduction of the Slit signal into the cytoskeletal rearrangement that accompanies a change in growth cone trajectory.

EXPERIMENTAL PROCEDURES

Site-directed mutagenesis

Oligonucleotide-directed mutagenesis was performed with a Promega in vitro mutagenesis kit to create the desired point mutations. Oligonucleotide primers were synthesized by the Caltech Oligonucleotide Synthesis Facility. The following oligonucleotide primers were used: DPTP10D–D1488A (cytoplasmic and full-length constructs), 5'-CACCTGGCCGGCCTTCGGTGTTCC; DPTP99A–D712A (cytoplasmic), 5'-CCAACTGGCCCGCCCACGGAACACC. Underlined bases are those that encode the mutant alanine residue. All mutations were verified by dideoxynucleotide sequencing performed by the Caltech DNA Sequencing Facility. The substrate trap version of DPTP69D, DPTP69D–D1065A, D1354A (DA3), was made by Paul Garrity at MIT. In this construct, alanine is substituted for the nonvariant aspartic acid in both phosphatase catalytic domains (D1 and D2).

S2 cell transfection, induction, harvesting and lysis

Growth medium used for S2 cells consisted of Schneider's medium supplemented with 10% heat inactivated fetal calf serum, penicillin (100 U/ml), streptomycin (100 μg/ml) and amphotericin B (0.25 μg/ml). 107 cells were plated on 10 cm tissue culture plates and expanded overnight (25º C, atmospheric pressure). Cells were transiently transfected with the DNA of interest (10 μg) using the calcium phosphate method. 18 hrs later the cells were washed with PBS and resuspended in growth medium. 0.3 mM $CuSO_4$ was added to induce the metallothionein promoter to drive expression. The cells were harvested 24 hrs later, washed in PBS and lysed in 450 μl of ice-cold lysis buffer (125 mM NaCl, 10 mM TrisCl pH 7.5, 0.2% Triton X-100, 600 μM PMSF, 2 mM Na3VO4, 25 mM NaF and

2 μg/ml APP). The lysate was spun briefly to pellet nuclei and insoluble membrane components.

Immunoprecipitations and Western blot analysis

Lysates were incubated with primary antibody and protein G+A agarose beads for 1 hr at room temperature. Robo was precipitated with mAbs provided by the Goodman lab. Myc-tagged proteins were precipitated with mAb 9E10. Agarose beads with bound immune complexes were spun down and washed with lysis buffer twice. Pellets were boiled for 3 minutes in SDS sample buffer. Samples were run on 9% polyacrylamide gels and transferred to a PVDF membrane. Blots were blocked in 5% dry milk in TBST (25 mM TrisCl pH 7.4, 137 mM NaCl, 0.2% Tween 20) for 30 minutes at RT. The blots were incubated in primary antibody for 1 hr, washed with TBST, and incubated with an alkaline phosphatase-conjugated goat anti-mouse secondary. After 30 minutes washing, the blots were developed to detect phosphatase activity. For Westerns, anti-pY mAb 4G10 (Upstate Biotechnologies), anti-myc mAb 9E10 and anti-Robo mAbs were used.

Figure 1. Molecular basis for substrate trap

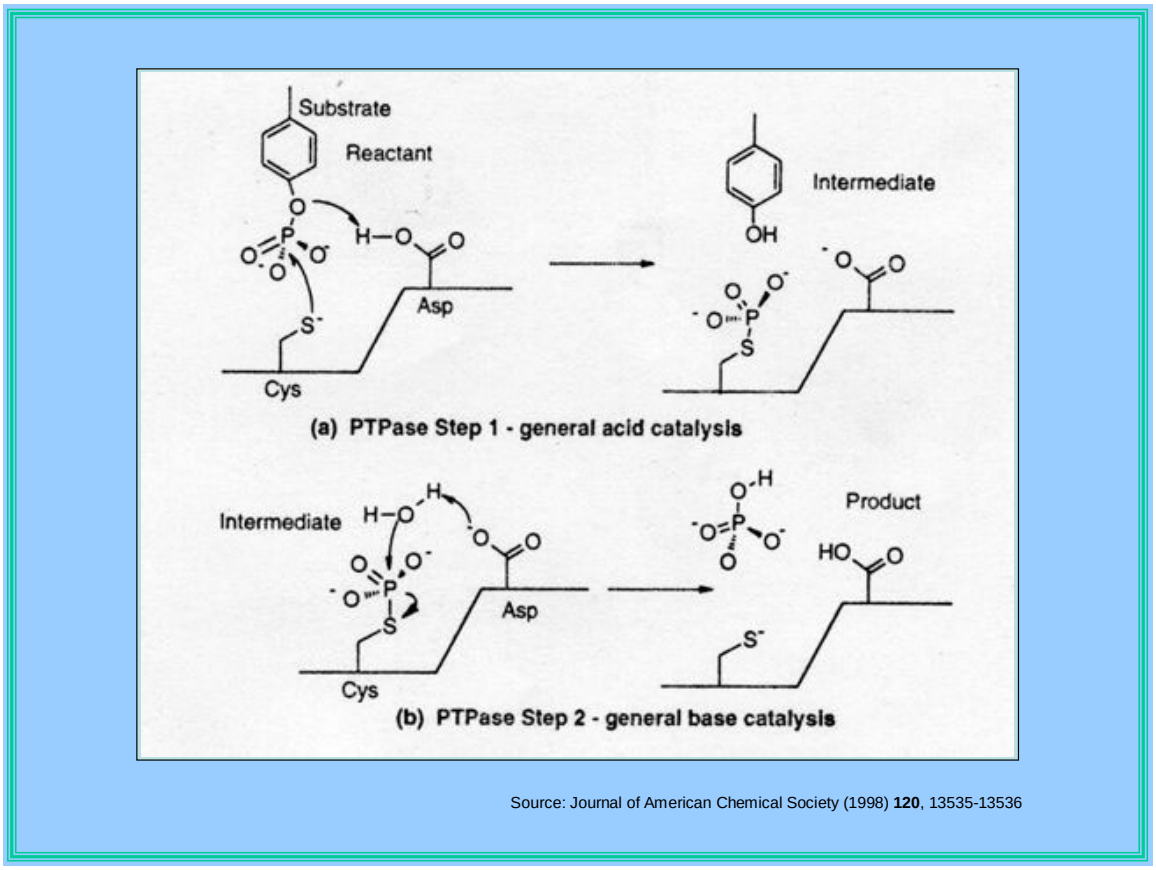

Source: Journal of American Chemical Society (1998) **120**, 13535-13536

Figure 2. Robo1 and Robo2 can be phosphorylated

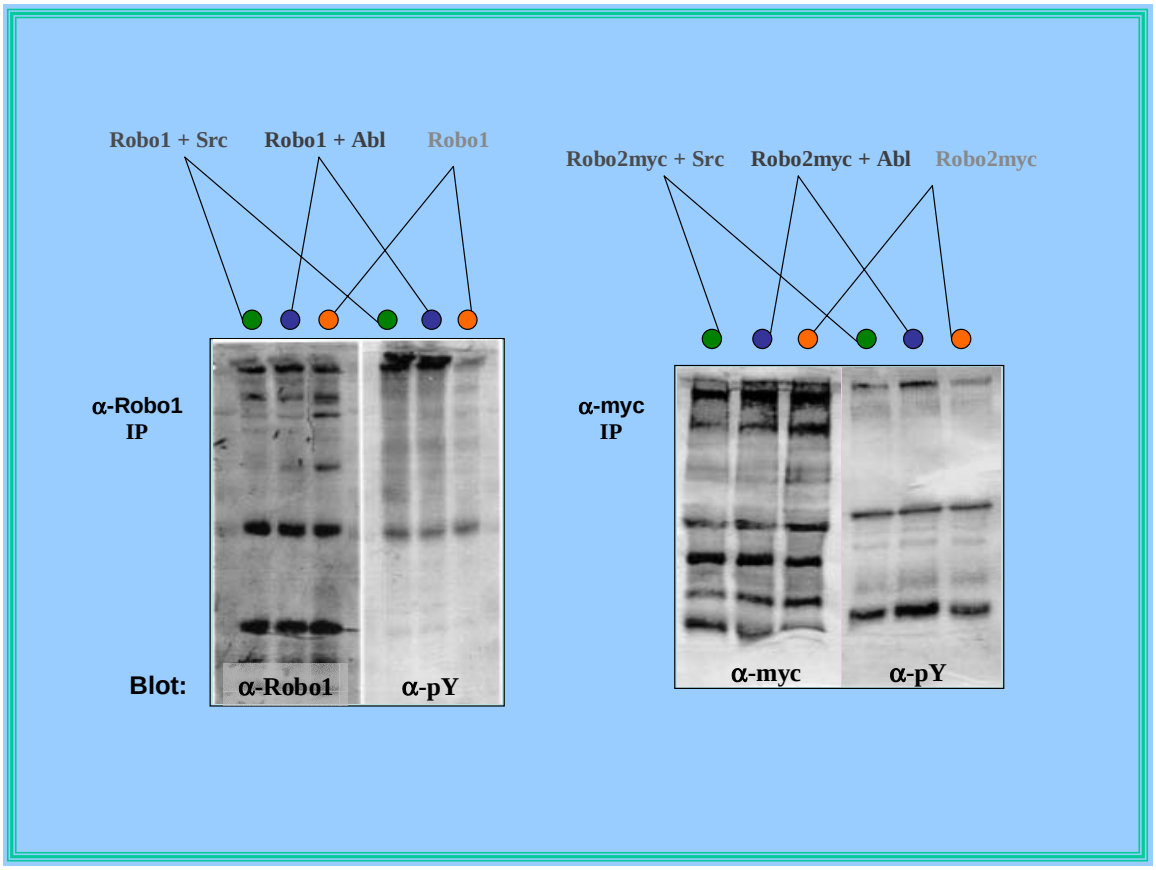

Figure 3. RPTP traps show little or no phosphorylation

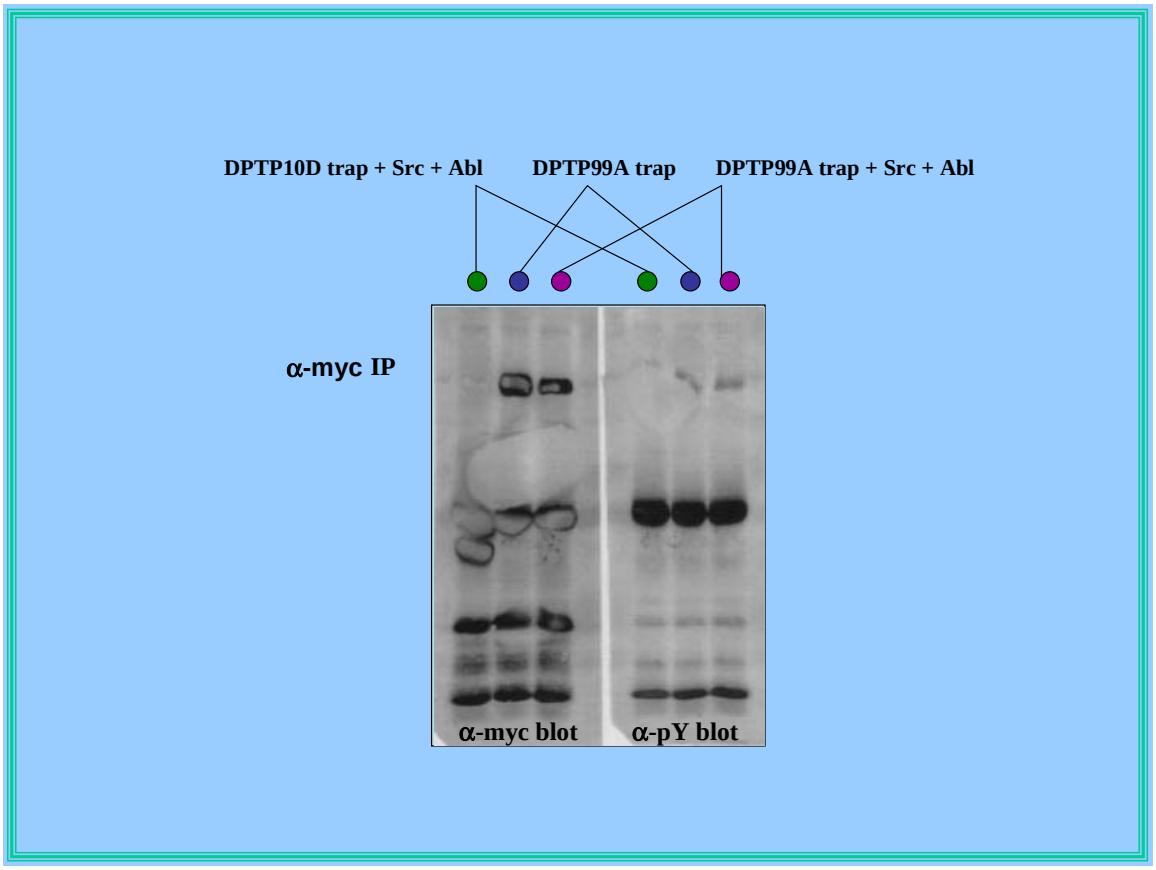

Figure 4. Robo1 cells transfected with DPTP10Dtrap, DA3 and Abl

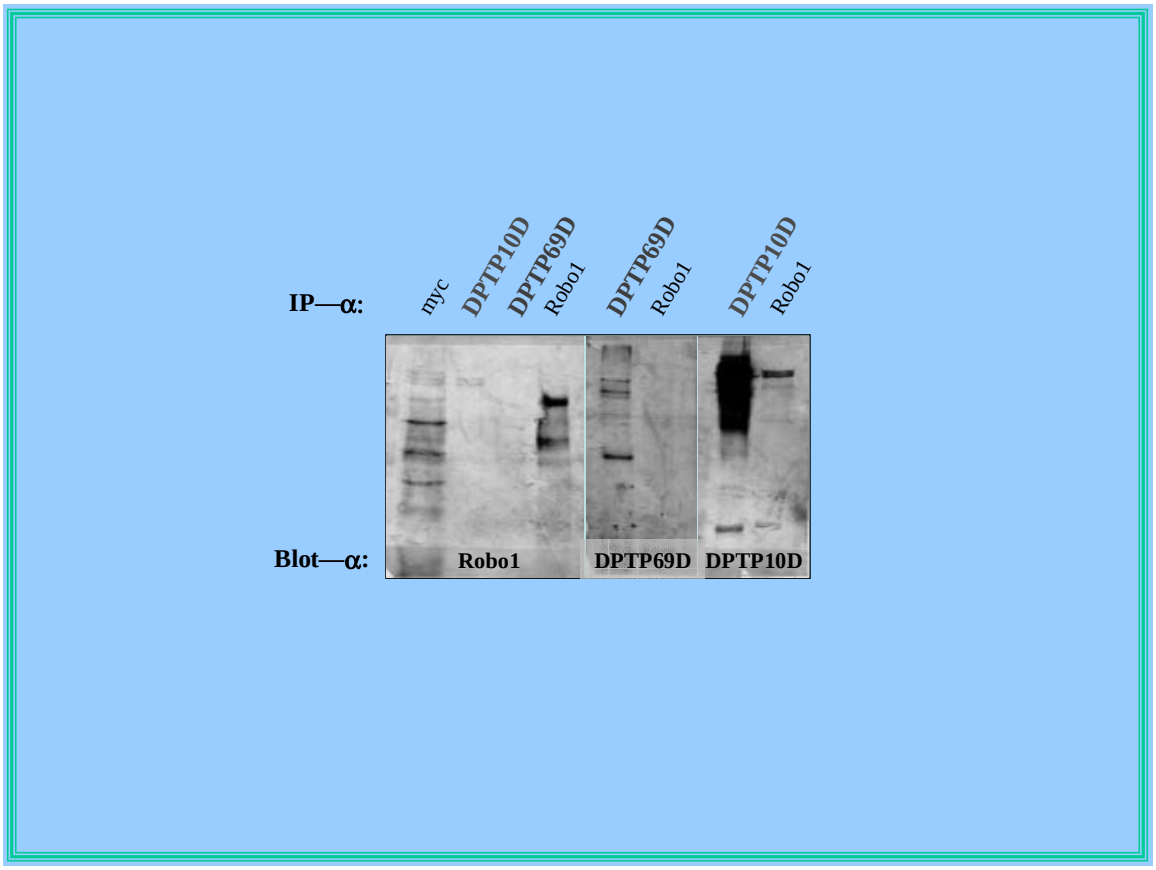

Figure 5. Robo2 cells transfected with Src and DPTP10D trap or DA3

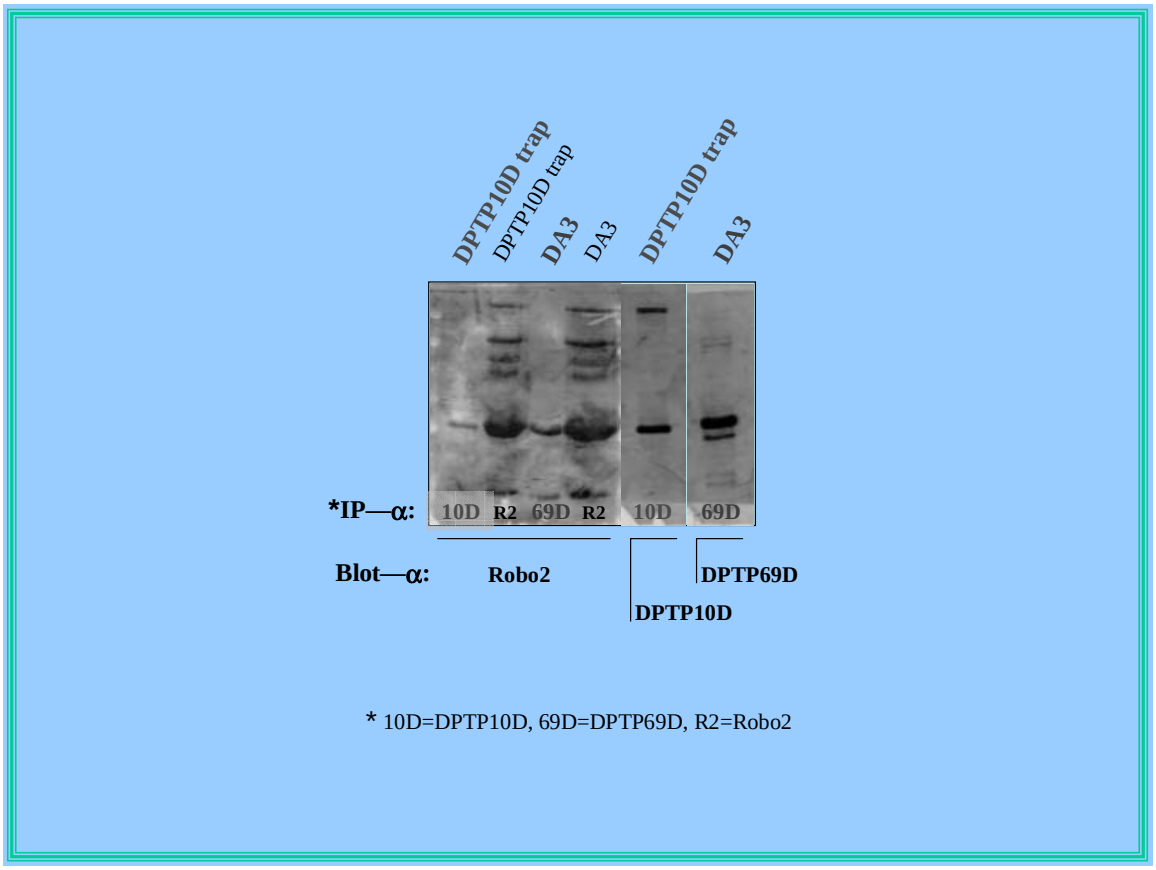

Figure 6. S2 cells transfected with DA3 and Abl, with or without Robo3

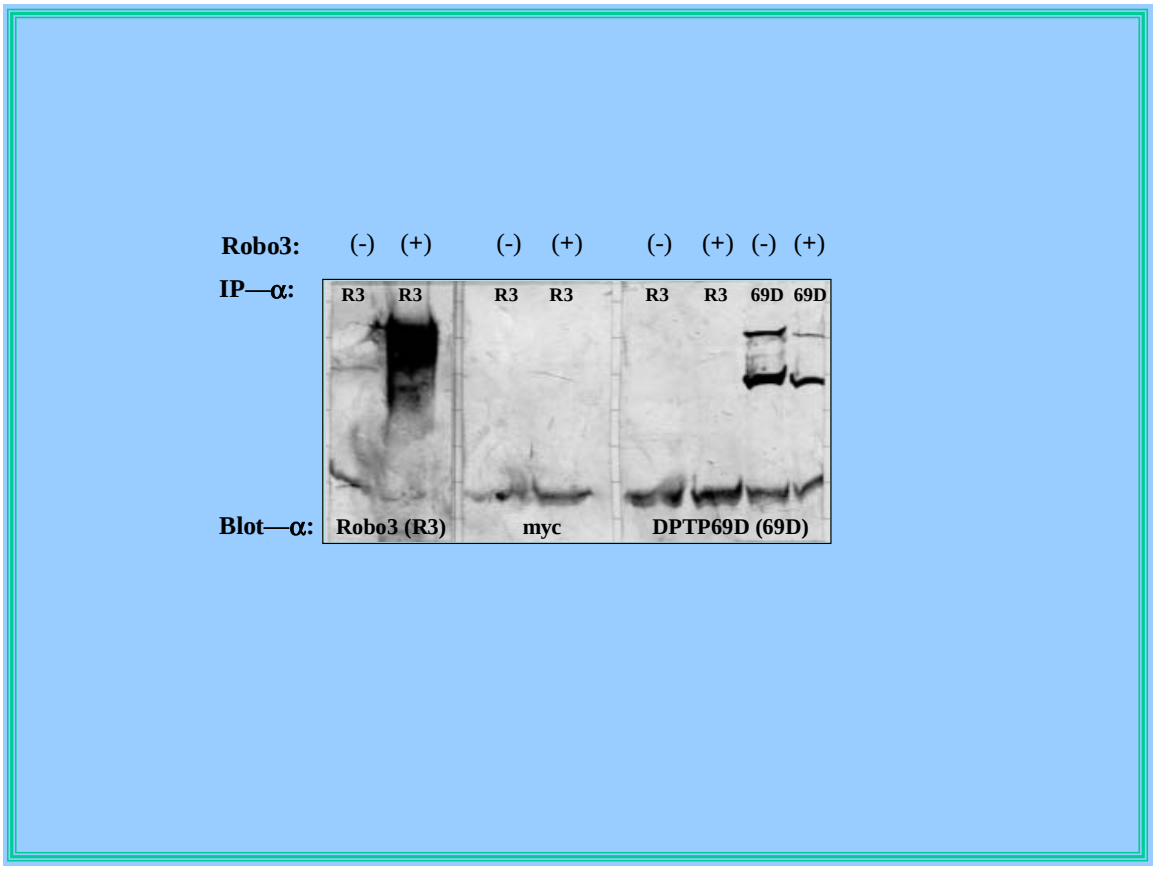

Table 1. Transfection experiments

S2 cells		
UAS Robo1 + Src (or Abl) + metallothionein GAL4 plus:	UAS Robo2myc + Src (or Abl) + metallothionein GAL4 plus:	UAS Robo3 + Src (or Abl) + metallothionein GAL4 plus:
DA3	DA3	DA3
DPTP10D trap FL myc	DPTP10D trap FL myc	DPTP10D trap FL myc
DPTP10D WT FL	DPTP10D WT FL	
DPTP69D WT FL	DPTP69D WT FL	
DPTP99A WT cyto myc		
DPTP99A trap cyto myc		
DPTP10D WT cyto myc		
DPTP10D trap cyto myc		

Robo1 cells
Src (or Abl) + metallothionein GAL4 plus:
DA3
DPTP10D trap FL myc
DPTP10D trap FL myc + DA3, induced with Slit cell media

Slit cells	
UAS Robo1 + Src (or Abl) + metallo-thionein GAL4 plus:	UAS Robo2 myc + Src (or Abl) + metallo-thionein GAL4 plus:
DA3	DA3
DPTP69D WT FL	DPTP69D WT FL

Chapter 4

Studies of proteins purifying with a “substrate trap” version of DPTP69D

Abstract

We have purified a “substrate trap” version of DPTP69D from transgenic flies and isolated several proteins that copurify with it. DA3 has a point mutation in an aspartic acid residue that causes it to remain bound to substrate. This is likely the basis for the axon guidance phenotype seen in flies expressing DA3. We purified DA3 from transgenic embryos overexpressing the mutant protein in the CNS. Two copurifying proteins were identified are members the protein disulfide isomerases (PDIs) family. PDIs assist in protein folding, but the relationship of these proteins to DPTP69D is as yet unclear. Mass spectrometry techniques were used to identify a third protein of 200 kD as non-muscle myosin II heavy chain (nmm II hc). Encoded by the *zipper* gene, nmm II hc plays a role in several developmental processes including axon patterning, dorsal closure and imaginal disc development. We show here that DA3 interacts with nmm II hc and yields a strong axon retraction phenotype similar to that caused by upregulation of nmm II activity when it is expressed in mushroom bodies, suggesting that DPTP69D may play a role in regulating nmm II activity.

INTRODUCTION

RPTPs play a pivotal role in axon guidance, the process by which a growth cones senses cues in its local environment and transduces them through a series of intracellular events into cytoskeletal changes. The dynamic restructuring of the cytoskeleton allows a growing axon to make trajectory changes needed to remain oriented towards its target destination. Four RPTPs are expressed selectively in *Drosophila* central nervous system (CNS) axons during axonogenesis (Desai et al., 1994; Tian et al., 1991), and mutations in these genes result in characteristic pathfinding defects (Desai et al., 1996; Krueger et al., 1996). Although much has been learned about the functional significance and genetic interactions among these RPTPs, little is known about the signaling pathway lying downstream of these enzymes. In hopes of elucidating this pathway we have attempted to identify phosphatase substrates using a substrate trap version of DPTP69D.

The RPTP phosphatase domain contains two amino acids essential for catalytic activity: a cysteine that acts as a nucleophile to initiate the dephosphorylation reaction, and an aspartic acid that acts as a proton donor to turn dephosphorylated substrate into a favorable leaving group (Zhang et al., 1994b). If the aspartic acid is mutated, catalysis terminates prematurely and the substrate remains attached to the RPTP (Flint et al., 1997). We exploited the trapping properties of this mutation to identify potential RPTP substrates.

A version of DTP69D with a trap mutation in both catalytic domains, denoted DA3, yields a strong CNS and motor axon phenotype when expressed at high levels. When stained with an antibody recognizing axons, embryos show an irregular nerve cord and motor axons that stop short of their target, ending in uncharacteristic club shapes (Figure 1). Overexpression of WT DPTP69D has no CNS phenotype and only a weak motor axon phenotype. The stronger phenotype in DA3 flies is likely the result of sequestration of one or more substrates by the trap.

To identify potential DPTP69D substrates we overexpressed DA3 in transgenic flies using the UAS/GAL4 system for tissue-specific gene expression (Brand and Perrimon, 1993). DA3 was purified on an anti-DPTP69D mAb column, and proteins that copurified were divided into three categories through comparison of results from other

purifications. Anything that purified with a control antibody was considered irrelevant and the result of non-specific binding to IgG. Proteins that copurified from both WT DPTP69D and DA3 flies were viewed as proteins that may interact with DPTP69D, and those that copurified exclusively with DA3 were considered potential substrates.

We sequenced and identified three proteins that interact with and/or are substrates for DPTP69D. Two are protein disulfide isomerases (PDIs) with an undetermined relationship to DPTP69D. A mutation in the third protein, non-muscle myosin II heavy chain (nmm II hc), results in a specific phenotype that is recapitulated by DA3 expression, suggesting nmm II hc may be a target of DPTP69D activity.

RESULTS

Females heterozygous for C155-GAL4 (driver line) were crossed to males homozygous for UAS DA3 (responder line, made by Paul Garrity at MIT). C155-GAL4 is an enhancer trap line that drives expression of GAL4 panneurally and is located near the ELAV gene. Stage 16 embryos from this cross were dechorionated and crushed into a powder in a liquid nitrogen-filled mortar. Subsequent purification of DPTP69D was done in collaboration with Peter Snow of the Caltech Protein Expression Center. Lysate prepared from the powder was applied to a concanavalin A (lectin) column to enrich for glycosylated surface proteins, and then split between two monoclonal antibody columns: 3F11 (anti-DPTP69D) for purification of DA3, and FA4 (anti-Neurotactin) to act as a control for nonspecific antibody binding. Material eluted from the columns was run on an acrylamide gel and transferred to a PVDF blot. Also included in the blot is one lane representing WT embryo powder purified on the 3F11 column. The three lanes in the final Coomassie stained blot are thus WT DPTP69D-3F11, DA3-3F11, and DA3-FA4 (Figure 2).

A band in the DA3-3F11 column absent from the other two columns represents a potential DPTP69D substrate. We found two such bands, with molecular weights of 66 and 44 kD. These PVDF-bound proteins were excised from the blot and sequenced using Edman degradation by Gary Hathaway of the Caltech PPMAL facility. The resulting N-

terminal sequence data led to their identification as CG's 9302 and 9911. A third band was present in both DA3 and WT 3F11 columns but absent from the FA4 column. If not a substrate, the specificity of the binding suggests it is at least a DPTP69D-interacting protein. At 200 kD this protein was too large for Edman degradation. We took an alternate approach that implements mass spectrometry to identify this protein as non-muscle myosin II heavy chain. Other smaller proteins less than 40 kD were obscured by a large quantity of yolk proteins, making it difficult to judge whether they were absent from the control antibody lane.

Two members of the PDI gene family copurify with DA3

Two proteins copurified with the trap version of DPTP69D but not its WT counterpart, suggesting they are potential substrates. Edman degradation of the larger protein (66 kD) yielded the following N-terminal sequence data: (Met, Lys)-Ser-(Xxx, Lys)-Thr-Ser-Ala-Val-Gln-Asp-Asp-Ile. Matching this sequence against those in the SWIS-PROT protein database led to identification of the protein as CG9302. The smaller protein (44 kD) was identified as CG9911 based on the sequence Ala-Gly-Ala-Val-Pro-Met-Thr-Ser-Asp-Asn-Ile-Asp-Met-Thr-Leu.

Interestingly, both proteins fall under the same functional category, namely protein disulfide isomerase (PDI). Both are orthologs of specific vertebrate proteins. CG9302 is an ortholog of human PDI-related (PDIR), whose function is unknown (Hayano and Kikuchi, 1995). It has two thioredoxin domains and one proline-rich domain. CG9911 is an ortholog of an uncharacterized human protein and closely related to another fly gene (CG10029). It has one thioredoxin domain and a C-terminal KDEL sequence (Lys-Asp-Glu-Leu). KDEL is an endoplasmic reticulum (ER) targeting sequence, which implies this protein permanently resides in the ER. In fact, we infer they are both ER proteins based on classic PDI (an ER protein). Both proteins have a signal sequence, while neither has a recognizable transmembrane domain.

These are two members of the large PDI gene family, whose members are involved in the processing and maturation of secretory proteins in the ER (Ferrari and Soling, 1999). They assist proteins in assuming the correct conformation by forming, isomerizing and reducing disulfide bonds. All PDIs contain at least one thioredoxin domain.

Thioredoxins are a class of small 12 kD proteins with a highly conserved active site containing two cysteine residues that can be reversibly oxidized to form an intramolecular disulfide bond. They participate in a variety of redox reactions and are present in all prokaryotes and eukaryotes.

Although PDIs are well characterized, the function of the two copurifying proteins is unknown as they do not correspond to the biochemically characterized PDI. As putative DPTP69D interacting proteins, we were interested in knowing whether they have a role in axon pathfinding. Accordingly, we looked for pathfinding defects in Bloomington line 10475, which has a lethal insertion near PDI of a P element with a lac Z reporter. Staining with mAb 22C10, which labels neuronal cells within the CNS and PNS, shows no irregularities. β-gal staining indicates PDI is expressed in salivary glands and peripheral neurons (Figure 3). RNAi experiments may provide more insight into the role of these proteins and their relation to RPTPs. However, we chose to pursue another protein from our purification experiment, as several considerations led us to believe it had more potential for interacting with DPTP69D in a physiologically significant manner.

Non-muscle myosin II heavy chain interacts with DA3

In the PVDF blot of eluates from the mAb columns, one band was present in both DA3 and WT lanes but absent from the control lane. This represents a protein that purifies specifically with DPTP69D but is not necessarily a substrate. The large size of this protein (200 kD) made Edman degradation impractical. Its identity was determined using an alternate technique that involves trypsinization of the protein and measurement of the resulting tryptic fragment sizes using mass spectrometry (performed by Gary Hathaway). The MASCOT program is then used to predict the protein's identity by matching it to proteins in the database that would yield the same array of fragment sizes upon trypsinization. In our case there was a strong prediction that the 200 kD protein was the non-muscle myosin II heavy chain (nmm II hc), encoded by the *zipper* gene. Subsequent Western blots using an anti-nmm II antibody confirmed the prediction.

In *Drosophila, zipper* is a single copy gene that is alternatively spliced at two sites (Mansfield et al., 1996). Similar to myosin II heavy chain in muscle, the nmm II hc protein is organized into head, neck and tail domains. The head domain includes a

nucleotide binding pocket and an actin binding sequence. The neck domain binds two light chain subunits, essential light chain (ELC) and regulatory light chain (RLC). nmm II is a hexamer comprised of two heavy chain subunits along with two subunits of both ELC and RLC. The activity of nmm II is controlled through phosphorylation of RLC, which in flies is encoded by the *spaghetti squash* gene (*sqh*) (Redowicz, 2001). Details of the *zipper* gene are shown in Figure 4.

To confirm the interaction of nmm II hc with DPTP69D, the purification experiment was repeated to see if it was reproducible. Using a 3F11 column to purify DPTP69D, we found nmm II hc copurifying for a second time. We corroborated this result by performing the experiment in a complementary manner, i.e., by purifying nmm II and probing for DPTP69D. nmm II hc's dimerize due to α-helical structures in the tail that associate to form a coiled-coil structure. The dimers polymerize via the tail domain, a characteristic that makes it possible to purify nmm II on a myosin II affinity column. This approach is necessary because the anti-nmm II mAb works well for Western blots but not for precipitations. After binding lysate from WT embryos to a column of myosin II-tail-coated beads (obtained from Dan Kiehart of Duke University), the column was washed and eluted with high salt. The eluate was run on an acrylamide gel and transferred to a PVDF blot. DPTP69D is visible when the blot is probed with 3F11, further evidence for a bona fide interaction (Figure 5).

To determine whether nmm II hc meets a primary tyrosine phosphatase substrate criterion, we sought evidence for phosphorylation on tyrosine residues. Lysate was prepared from a cross of C155-GAL4 and UAS DA3 embryos, and myosin-coated beads were used to precipitate nmm II. Using an anti-phosphotyrosine polyclonal (anti-pY) antibody, we were unable to detect an nmm II hc band in the precipitate. Probing with anti-myosin indicated the precipitation of nmm II hc was weak. Furthermore, only a small fraction of our precipitate was likely to have been neuronal nmm II, as myosin is prevalent in many cell types, with the vast majority in cells other than neurons. To address this problem we used larval CNS/imaginal disc extracts (approximately 60 larvae) that are greatly enriched for neurons. Probing with anti-myosin showed a solid nmm II hc band, but anti-pY indicated none was phosphorylated. In the event that nmm II hc was being dephosphorylated by a phosphatase present in the lysate, we added 1 mM sodium

orthovanadate to the lysis buffer to inhibit phosphatases. Repeating the experiment under these conditions did not affect the outcome.

In a general assay of the effect of *zipper* mutations on axon pathfinding, we stained several *zipper*- lines with mAb 1D4, an anti-Fascilin II mAb that recognizes all motoneurons and a subset of CNS axons. The overall structure of the CNS and PNS looks normal in embryos from these lines (Bloomington stock numbers 2528, 4199 and 11215 and three alleles provided by the Kiehart lab).

DA3 expression in leading edge cells does not perturb dorsal closure

nmm II plays an integral role in several morphogenetic processes during *Drosophila* embryonic development (Young et al., 1993). We sought to determine whether expression of DPTP69D trap would interfere with any of these processes. If an interaction does exist, the properties of the trap are such that it should sequester nmm II, thereby disrupting biological events that depend on its function.

An example of one such event is dorsal closure, the process in which the epithelial walls of the embryo elongate and eventually meet and fuse at the dorsal midline to generate a continuous dorsal epidermis. A specialized group of cells in the dorsal-most row of the lateral epithelia on each side of the embryo, called leading edge (LE) cells, are required to orchestrate closure. nmm II and actin are asymmetrically localized to the apical side of the LE cells, where they form a contractile band. Because the LE cells are mechanically linked, actomyosin based contraction of this band has an effect similar to tightening a purse string. This in turn draws the lateral epidermis towards the dorsal midline to effect closure.

In strong *zipper*- alleles, dorsal closure never takes place, evidence for the essential role of nmm II hc in mediating this process (Stronach and Perrimon, 2001). In weaker alleles, closure is arrested at intermediate stages or simply delayed. To test whether expression of DA3 would result in similar closure abnormalities, we drove expression of DA3 in LE cells. We crossed homozygous UAS DA3 females to heterozygous puc^{E69}; pnr GAL4 males. pnr drives expression of GAL4 in a region encompassing LE cells, and puc^{E69} is a P element enhancer trap in the puckered locus that expresses lac Z in leading edge cells (this line was provided by the Perrimon lab at Harvard). β-gal is detectable

from the start of dorsal closure at stage 13 until the end of closure at stage 16, when LE cells have formed the dorsal midline.

We stained appropriately staged embryos from this cross with anti-myc to confirm DA3 expression, and with anti-β-gal to visualize LE cells. No evidence of dorsal closure irregularities was observed.

DA3 expression in mushroom body neurons yields axon retraction phenotype

Another developmental process in which nmm II plays an essential role is mushroom body (MB) development. The MB is a specialized structure in the insect brain implicated in olfactory learning and memory. All insects have two MBs, one on each side of the midline. The adult MB is comprised of three types of axons: γ, α'/β' and α/β. The early born γ neurons project only medially, but the later born α'/β' and α/β neurons bifurcate anteriorly, each projecting one branch dorsally and the other medially towards the midline.

nmm II's role in MB development was elucidated recently when it was found to be a key component of an axon retraction pathway in this brain structure (Billuart et al., 2001). The pathway is normally repressed by a RhoGAP called p190, but when the activity of p190 is suppressed a sequence of events culminating in axon retraction ensues. The ultimate output of this pathway is nmm II, specifically the regulatory light chain encoded by *spaghetti squash* (*sqh*). In embryos expressing p190 dsRNA, the dorsal branch of the MB is truncated to varying degrees. When a null mutation in *sqh* is introduced into this background, the phenotype is markedly suppressed. This suggests that the *p190* mutant phenotype is due to overactivity of nmm II. Consistent with this, introduction of a phosphomimetic *sqh* mutation enhances the *p190* phenotype. Taken together, these data suggest that nmm II activity regulates axon extension/retraction in MBs.

To test if DA3 expression produces an MB axon extension/retraction phenotype consistent with alteration of nmm II activity, we crossed UAS DA3 flies to an MB GAL4 source. Homozygous UAS DA3 females were crossed to males homozygous for UAS CD8 GFP; OK107-GAL4. The OK107 driver expresses GAL4 in all mushroom body

neurons, which in turn drives localized expression of DA3 and a built-in reporter. The reporter, green fluorescent protein (GFP), is targeted to the plasma membrane by the CD8 receptor transmembrane sequence. This allows visualization of all axonal and dendritic projections of MB nerve cells. (This line was provided by the Luo lab at Stanford.) The temperature dependence of GAL4 expression makes it possible to assay whether a given phenotype is stronger in flies crossed at higher temperatures (where expression is strong) relative to flies crossed at lower temperatures (weaker expression). Thus, both crosses were performed at two different temperatures, 25º C and 29º C. To serve as a control, we crossed the same GAL4 driver line to UAS μ/DPTP69Dmyc flies, again at both temperatures. The μ/DPTP69Dmyc chimera consists of the extracellular and first 57 amino acids of intracellular RPTPμ fused to the intracellular domain of DPTP69D, with a myc tag at the C terminus.

MBs were dissected from adult flies and viewed directly or fixed and stained with anti-GFP. There is a strong axon retraction phenotype in the MBs of trap mutants (Figure 6). The most striking feature of the phenotype is the absence of the dorsal branch. In flies raised at 25º C the dorsal branch is missing from most of the samples examined, and in flies raised at 29º C it is missing in all samples. Additionally, the medial branch often appears foreshortened or distorted. The MB calyx is a neuropil comprised of the dendritic arborizations of the MB neurons, known as Kenyon cells. Calyces of trap mutants often appear smaller than normal or exhibit an irregular morphology. A missing dorsal branch is sometimes observed in the cross with the RPTP chimera, suggesting that its activity differs from that of WT DPTP69D in a way that leads to a similar phenotype, albeit at a much lower frequency. This is in contrast to the driver line crossed to itself, where in all embryos examined the MBs are normal in every respect. The phenotype of the trap mutants closely resembles the *p190* mutant phenotype reported by the Luo lab, suggesting that perturbation of nmm II activity regulation may be the basis for the DA3 MB phenotype.

DISCUSSION

The in vivo approach to isolation of potential enzyme substrates has several advantages over an in vitro approach, where lysate from a neuronal cell line is applied to an antibody column. In the embryo, a full complement of potential substrates is expressed, whereas a cell line expresses only an undetermined subset. Candidate substrates can be transfected into cells, assuming they are available in suitable expression vectors, but other issues make this a less than ideal solution. In embryos, all substrates are expressed at the appropriate stage of development and localized to the correct part of the cell. This stands in contrast to the cell line, where expression is induced at a chosen time point and cell localization is likely arbitrary in many cases. In the in vivo approach, which substrate residues are phosphorylated, the timing of the phosphorylation and the kinases that catalyze the reaction all reflect normal physiological conditions. Conversely, with a cell line one must transfect a kinase if it is not expressed endogenously and hope that it phosphorylates the appropriate substrate residues.

The *Drosophila* genome sequence was completed in March of 2000, and our experimental design exploits the recent availability of this sequence. Putative substrates are isolated with a phosphatase trap, and then identified by obtaining N-terminal sequence data and searching the genome. For DPTP69D we have identified two copurifying proteins whose relationship to the phosphatase is unclear. We have also identified non-muscle myosin II heavy chain, which interacts with DPTP69D and is implicated in regulating axon branch stability in the insect mushroom body.

PDIs are unlikely substrates for DPTP69D

Two proteins of 44 and 66 kD that copurify with DA3 are categorized functionally as protein disulfide isomerases (PDIs). PDIs are small proteins that typically reside in the ER and are present in all prokaryotes and eukaryotes. Together with chaperones they regulate protein folding, a process that is not instantaneous but takes place over seconds or minutes. Chaperones cover sticky regions of the protein that would otherwise cause aggregation, while PDIs assist in forming and rearranging disulfide bonds among and

within polypeptides until a proper conformation is reached. The sequence of the 66 kD protein (CG9302) aligns very well with human PDIR (e^{-102}), but is not very close to human PDI itself (e^{-18}). The 44 kD protein (CG9911) is closely related to an uncharacterized human protein (e^{-100}) and to another fly protein (CG10029).

These PDIs are implicated as substrates for DPTP69D because they purify with a trap version of DPTP69D and not the WT enzyme. Since the proteins they most closely align with have an unknown function, it is possible to ascribe to PDIs an as yet undefined signaling role. However, several considerations militate against assigning this function to PDIs. Foremost among them, PDIs generally reside in the ER while the phosphatase domain of the RPTPs is in the cell cytoplasm. This disparate cellular location would preclude an interaction. Some PDI-related proteins have been reported to localize to the cell surface, but the ones we have identified have a signal sequence and no transmembrane or cytoplasmic domain. Indeed, CG9911 has an ER retention sequence so it almost certainly resides in the ER. Second, there is no evidence either of these PDIs is phosphorylated on tyrosine residues, a necessary prerequisite for an RPTP substrate. Third, an alternate explanation for the association exists that is perhaps more compelling.

One possibility for why these proteins purify with the trap version of DPTP69D but not WT is that the trap mutant may be incapable of folding well. The PDIs may have been isolated as a by-product of their prolonged association with partially folded protein. If this were the case the DA3 phenotype could be attributed to the inability of misfolded DPTP69D to make it out to axons. To test this hypothesis, we stained DA3 embryos with anti-myc to visualize the distribution of trap protein. The staining indicates the trap mutant does make it into axons, although it remains possible the amount making it out is less than normal. Cell bodies are visible, but a conclusion that mutant protein is getting held up in cell bodies cannot be drawn. It is more likely a by-product of overexpression, as cell body staining is frequently seen in overexpression embryos.

DA3 overexpression produces a strong mushroom body axon retraction phenotype similar to that of *p190 RhoGAP* mutants

A 200 kD protein purifying with WT and trap DPTP69D but not control antibody was identified as non-muscle myosin II heavy chain (nmm II hc) and shown to interact with

DPTP69D in precipitation assays. nmm II hc, encoded in *Drosophila* by the single-copy *zipper* gene, plays a role in several developmental processes, including axon patterning, dorsal closure and imaginal disc development (Edwards and Kiehart, 1996; Zhao et al., 1988). The UAS/GAL4 system was used to target expression of DA3 to cells that play a role in two such processes. Dorsal closure is effected by a row of interconnected leading edge (LE) cells when apically localized nmm II contracts, causing them to elongate upwards until they cover the dorsal surface of the embryo. We expressed DA3 in LE cells but saw no evidence for any obvious dorsal closure irregularities. In contrast, when DA3 is expressed in the Kenyon cells that comprise the MB a strong axon patterning phenotype is observed.

MBs are prominent structures in the insect brain that integrate information from several modalities (visual, mechanosensory and olfactory) to mediate learning and memory. Each of the two bilateral MBs is comprised of approximately 170,000 Kenyan cells whose axonal projections originate in the calyx and project in bundles into the midbrain. En route to the midbrain each axon bifurcates, projecting one branch medially and the other dorsally.

A signaling pathway was recently elucidated that regulates a dynamic process of extension and retraction of MB axons (Billuart et al., 2001). RNAi inactivation of RhoGAP p190 causes an axon retraction phenotype manifested in shortened or absent dorsal braches. RhoA overexpression in this background enhances this phenotype, and expression of a constitutively active form of Drok phenocopies p190 inactivation. Biochemical and genetic studies suggest that a key output for Drok is MRLC, the regulatory light chain of nmm II encoded by the *spaghetti squash* (*sqh*) gene (Winter et al., 2001). These results suggest a model whereby RhoGAP inactivation leads to increased RhoA activity, which in turn activates the RhoA associated kinase Drok. Phosphorylation of MRLC causes increased actomyosin contractility resulting in axon branch retraction. This model is supported by the observation that the p190 inactivation phenotype is largely suppressed by removal of one copy of *sqh*.

Our results indicate that overexpression of DA3 in MBs results in a phenotype similar to that seen in *p190* mutants, only stronger. Dorsal branches are missing entirely in a majority of DA3 embryos, with none of the “weak” or “medium” phenotypes

observed in *p190* mutants. A feature common to both mutants is the presumptive involvement of nmm II, leading us to speculate that the DA3 phenotype may also be due at least in part to misregulation of nmm II activity. In the case of *p190* mutants, increased phosphorylation of RLC causes a corresponding increase in nmm II activity. Our purification experiment suggests the nmm II heavy chain is a substrate for DPTP69D. No examples of regulation of nmm II activity through phosphorylation of its heavy chain have been documented. Evidence does exist for phosphorylation of the heavy chain on tyrosine residues (Mishra-Gorur and Castellot, 1999). However, we were unable to detect tyrosine phosphorylation in the fraction of nmm II hc that copurifies with DPTP69D.

The absence of detectable phosphorylation in nmm II hc and the observation that it copurifies with both trap and WT versions of DPTP69D implicate it as a protein that interacts with DPTP69D but is not a substrate for this enzyme. In that case, how may DPTP69D be involved in regulation of nmm II activity? We envision a model in which DPTP69D binds both nmm II and an as yet unidentified substrate that is a negative regulator of nmm II. In a WT embryo, the substrate would bind DPTP69D and be dephosphorylated, at which time it would downregulate activity of the complexed nmm II. In this scenario, DPTP69D has a dual function, serving to activate a putative substrate enzyme through dephosphorylation, and to localize the protein (nmm II) on which the enzyme acts. DA3 has a point mutation near the phosphatase domain active site that should not interfere with its nmm II binding function. The substrate activation function would be compromised, however, since the dephosphorylation reaction does not occur. With the presumptive inhibitor of nmm II inactive, abnormally high levels of nmm II activity would result and lead to axon retraction. This could be the basis for DA3's other phenotypes as well, as the stalling and gaps observed in CNS axons and the premature termination of PNS axons could be the result of nmm II overactivity.

Since the above model invokes a mystery substrate, it would be reasonable to wonder why such a substrate was not identified in the purification experiment. One possibility is that it was obscured by yolk protein. Embryo purifications are complicated by the high levels of yolk protein, and methods for increasing the purity of the preparation (such as the ConA column used in this study) are only so effective. If the protein in question were smaller than 40 kD, it would have been in the midst of a smear

of yolk proteins. We sequenced only discrete bands that were absent from the control antibody lane, criteria that effectively eliminated everything under 40 kD.

In light of the fact that some substrates may have eluded isolation in our purification, the possibility remains that the DA3 phenotype is due to sequestration of a protein unrelated to the actomyosin system, and that the interaction between DPTP69D and nmm II hc is physiologically irrelevant. To sort this out, we intend to perform genetic interaction experiments. Specifically, we will remove one copy of either *zipper* or *sqh* in flies with MB-targeted DA3 expression to see if the associated axon retraction phenotype is suppressed.

EXPERIMENTAL PROCEDURES

Preparation of embryo powder

Embryos were collected at the appropriate stage (15-16), dechorionated with 50% bleach for 5-10 minutes, and rinsed with di-H_2O. Dechorionated embryos were ground into powder using a mortar and pestle partially filled with liquid NO_2 (LN2). Additional LN2 was added as needed during the grinding process to ensure the powder remained frozen at all times. When grinding was completed, the powder/LN2 mixture was poured into a conical tube on ice. The tube was transferred to a -80º C freezer with the cap loose to allow remaining LN2 to slowly boil away. Powder was kept at -80º C until an amount sufficient for the purification experiment had been collected (approximately 10 grams).

Purification of DA3

Peter Snow (Caltech Protein Expression Facility) prepared lysates from DA3 and WT DPTP69D embryo powder using a buffer comprised of 100 mM NaCl, 20 mM TrisCl (pH 8.0), 1% triton X 100 and 0.1% deoxycholate (DOC). The lysis buffer was supplemented with the following protease inhibitors: 1 mM EDTA, 1 µM Leupeptin, 1 µM Pepstatin, 1 mM phenylmethylsulfonyl fluoride (PMSF) and 1 µg/ml aprotinin. Embryo powder was homogenized by douncing six times with a Teflon pestle in a 2 ml

dounce. Homogenized material was incubated on ice for 30 minutes, vortexing every 5-10 minutes, then spun in a micro centrifuge for 10 minutes at 4º C to pellet nuclei and insoluble membrane components.

Lysates were first applied to concanavalin A (ConA) columns to achieve a roughly 10-20 fold enrichment in cell surface proteins. Eluate from the DA3-loaded ConA column was added to two mAb columns: mAb 9E10 (anti-myc, to purify myc-tagged DA3 and any associating proteins), and mAb FA4 (anti-Neurotactin, to control for non-specific binding to IgG). Eluate from the WT DPTP69-loaded ConA column was added to a mAb 3F11 column (anti-DPTP69, to identify proteins that copurify with DPTP69D independent of the trap mutation and are hence not likely to be substrates). Following several washes bound protein was eluted from the columns and run on an SDS polyacrylamide gel. Protein was transferred from the gel to a PVDF filter and stained with Coomassie blue.

Identification of copurifying proteins

Coomassie blue was used to stain a PVDF filter prepared by Peter Snow containing DPTP69D and DA3 in separate lanes, along with their corresponding copurifying proteins. Bands representing potential substrates were cut directly out of the filter and given to Gary Hathaway (Caltech Protein/Peptide Microanalysis Facility). N-terminal sequence data was obtained via Edman degradation for a 66 kD protein: (Met, Lys)-Ser-(Xxx, Lys)-Thr-Ser-Ala-Val-Gln-Asp-Asp-Ile, and a 44 kD protein: Ala-Gly-Ala-Val-Pro-Met-Thr-Ser-Asp- Asn-Ile-Asp-Met-Thr-Leu. These proteins were identified as CGs 9302 and 9911 through a search of the SWIS-PROT protein database.

Because Edman degradation is less efficient with larger proteins, an alternate approach was taken for identification of a third protein of 200 kD. Gary Hathaway digested the protein with trypsin and put tryptic peptides through a mass spectrometer to separate them by molecular weight. Out of a total of 335 peptides, the molecular weight of 19 could be resolved with a high degree of accuracy. Of these, 17 match nmm II hc based on a prediction made by MASCOT, a program that compares the array of fragment sizes to a database of tryptic fragment size arrays of known proteins. This prediction was later confirmed by Western blot analysis using an anti-nmm mAb (GP #12).

Immunohistochemistry and microscopy

Bloomington line 10475, a lethal P element insertion near PDI, was stained with mAb 22C10, labeling postmitotic neurons within the PNS and CNS. β-gal from the P element was stained with the anti-β-gal mAb 40-1a to visualize expression pattern. Embryos from a cross of puc^{E69}; pnr GAL4 to UAS DA3 were stained with anti-myc mAb 9E10 to confirm DA3 expression, and with mAb 40-1a to visualize LE cells expressing β-gal. Stage 16 DA3 and *zipper*- embryos were stained with the anti-Fasciclin II mAb 1D4, which labels a subset of longitudinal fascicles and all motor axons.

Adult flies were anaesthetized with CO_2 and put into 95% EtOH. Dissections were performed in cold PBS. Dissected fly brains were placed in Equilibration Buffer (Component C of Molecular Probe's SlowFade Antifade Kit) for approximately 10 minutes, and transferred to SlowFade Antifade reagent (Component A). The brains were mounted in Antifade reagent and imaged directly using a confocal microscope with a 488 nm laser. The signal was just as strong as when using an anti-GFP mAb and a fluorescent secondary (AlexaFluor 488).

Figure 1. DA3 embryonic phenotype

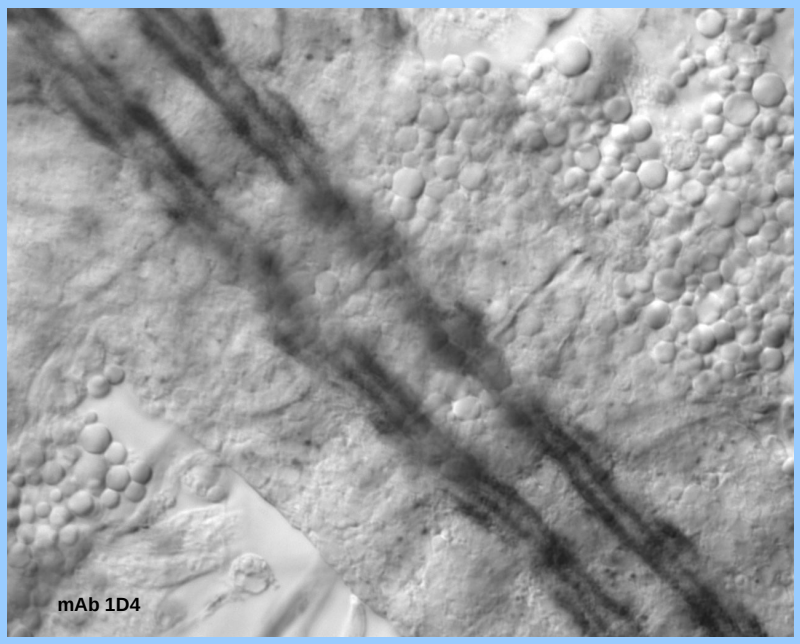

CNS: irregular nerve cord. **Motor axons**: SNb ends in club, ISN stops short.

Figure 2. Eluate blot

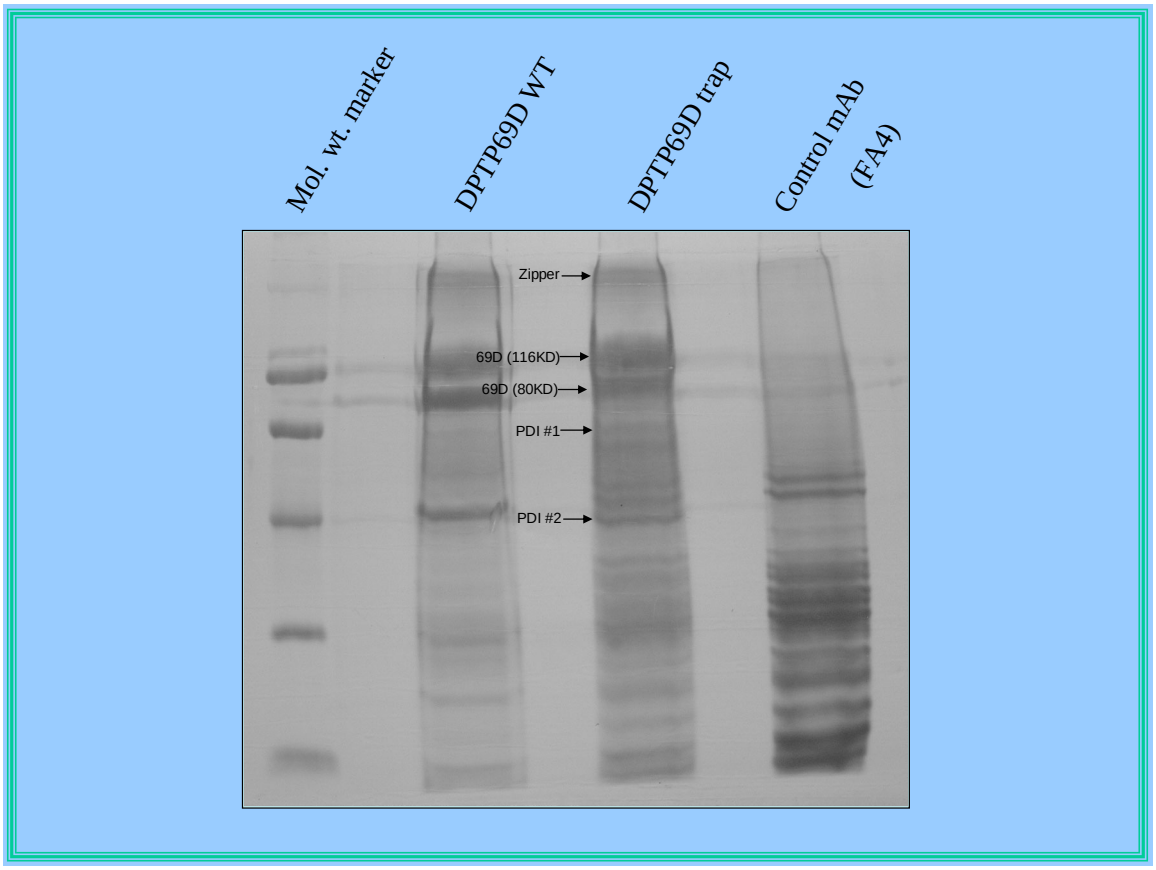

Figure 3. Examination of Bloomington line 10475 (lethal P element insertion near PDI). No obvious axon pathfinding defects.

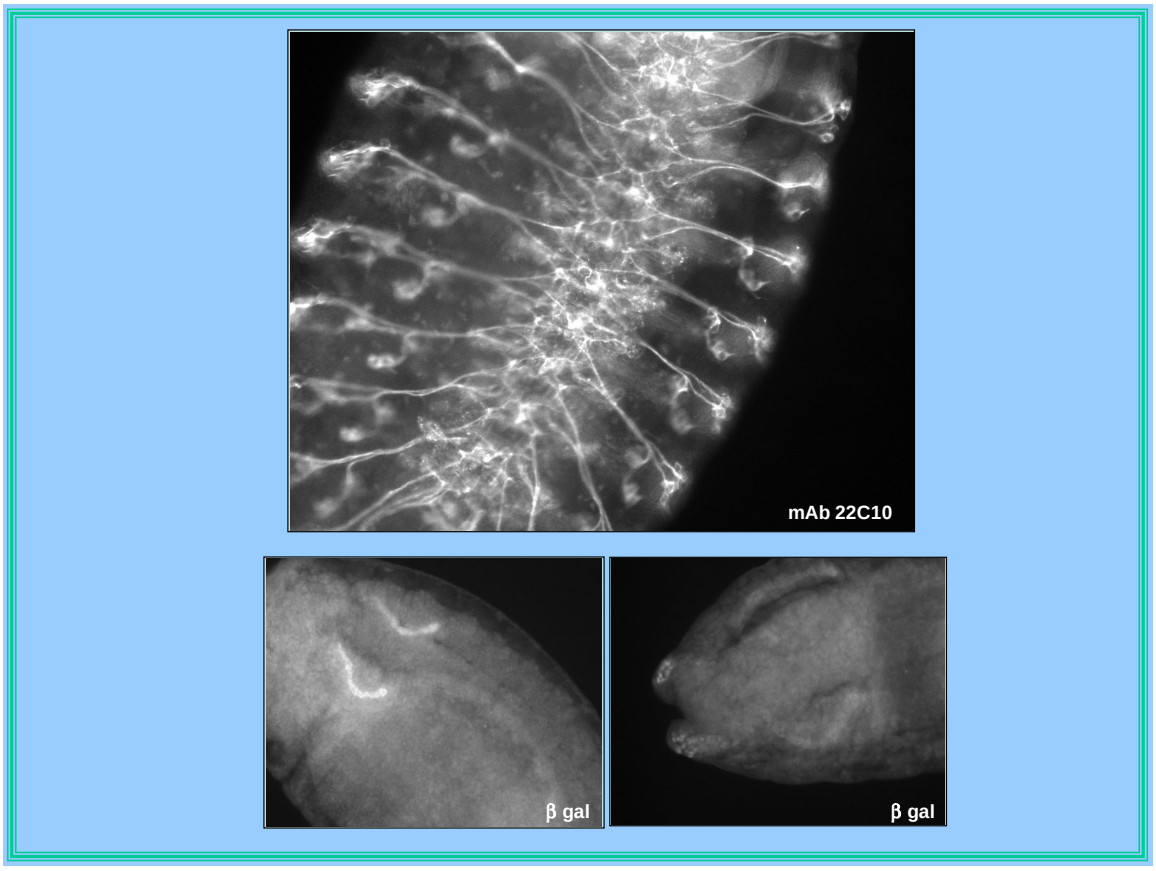

Figure 4. *zipper* schematic

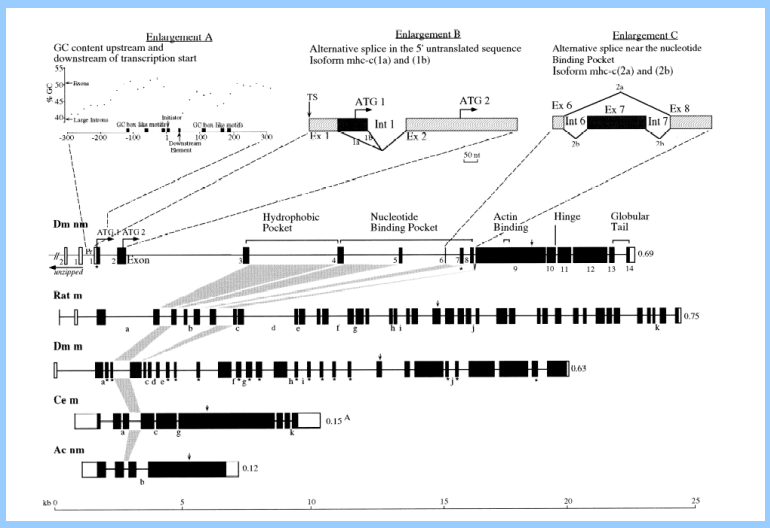

Figure 4. A schematic diagram depicts the overall genomic organization of the *Drosophila* non-muscle MHC gene, compares it to five other MHC gene structures that have been described and compares conservation of intron position throughout phylogeny. References for myosin sequences are shown in Table 1. The genes are aligned with respect to their methionine initiator codon; the *Drosophila* gene has two potential start sites as shown (ATG). Untranslated sequence is shown as open boxes, coding sequence as filled boxes and introns as thin lines. Alternative exons are marked with an asterisk. Intron boundaries conserved between all five genes or between *zipper* and another gene are shown with shading. Boundaries conserved between genes other than *zipper* are indicated with the lower case letters a through *k*. Boundaries were considered to be conserved between different myosins if the sequence immediately preceding or following a boundary was well conserved. Arrows show the N-terminal end of the tail. Numbers at the end of each gene represent the intron sequence as a fraction of the total sequence (transcription start to the poly(A) addition signal). Note that there is a progressive reduction in the number and total amount of intron in MHC genes in less complex species. Dm nm, *D. melanogaster* non-muscle (*zipper*); Rat m, rat (embryonic) skeletal muscle; Dm m, *D. melanogaster* muscle; Ce m, *Caenorhabiditis elegans* body wall muscle (*unc-54*); Ac nm, *Acanthamoeba castellanii* non-muscle. Detailed views of the promoter region and the two alternative splice sites in *zipper* are shown in the enlargements A to C above the genomic structure. A, Schematic representation of the promoter region in the *Drosophila* non-muscle MHC gene shows a progressive increase in GC content from -300 to transcription start and the presence of GC box-like motifs. The GC content values for the region -1 to -300 were calculated in a cumulative fashion beginning at -1 and proceeding upstream in bins of 20 nt. The same procedure was used for the region +40 to +300 beginning at +40 and proceeding downstream. B and C, Shaded boxes indicate sequence that is only present in the isoform mhc-c(1b) and mhc-c(2b), respectively. Hatched boxes indicate the sequences common to both classes of transcript. Pr, putative promoter region; TS, transcription start.

Source:Journal of Molecular Biology (1996) **255**, 98-109

Figure 5. nmm II hc purification from WT embryos

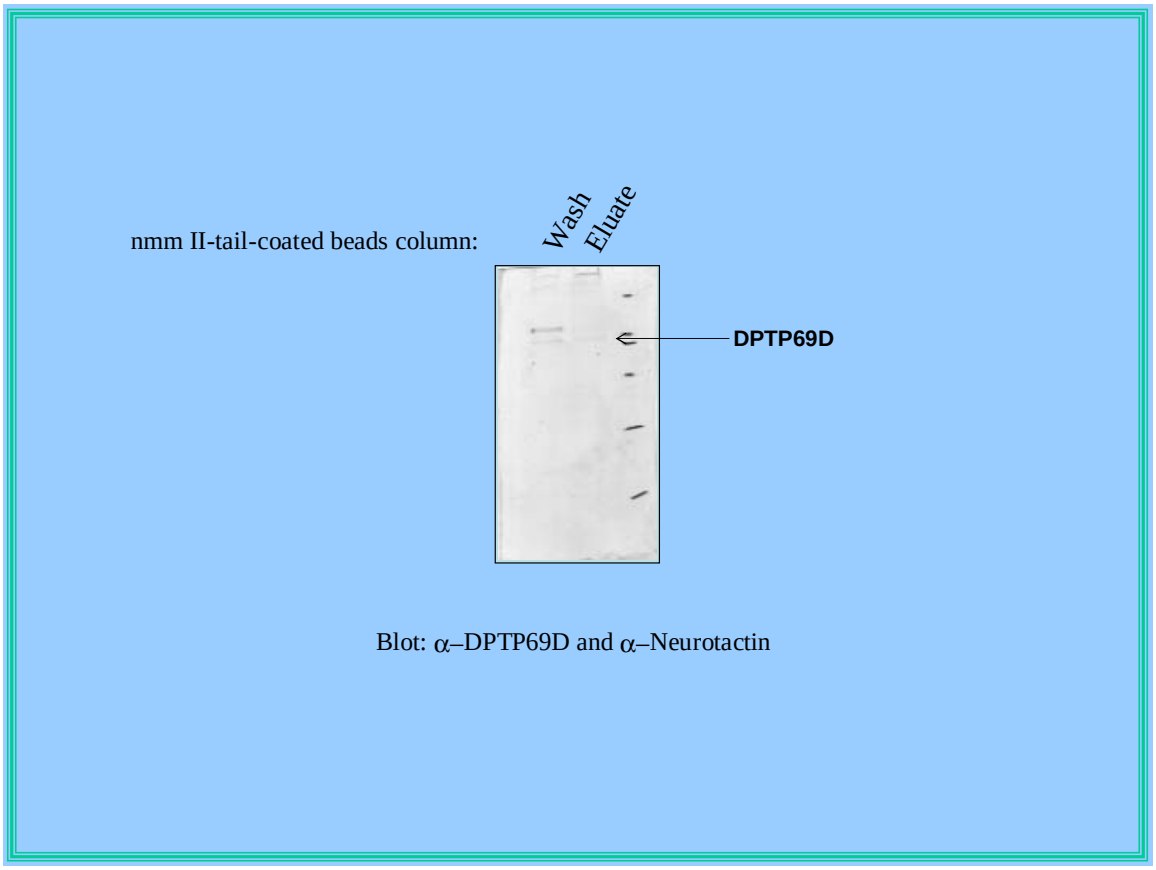

Figure 6. DA3 expressed in MB causes axon retraction phenotype

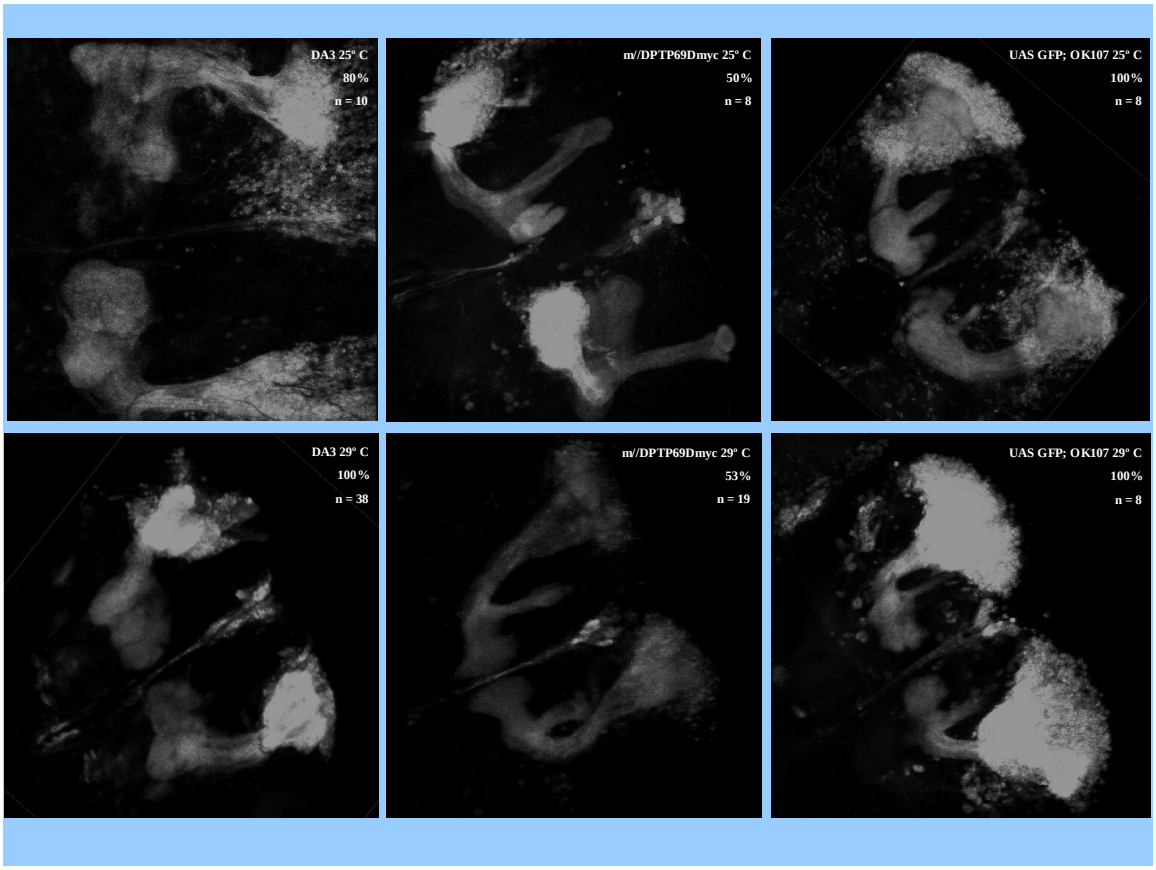

References

Barford, D., Das, A. K., and Egloff, M. P. (1998). The structure and mechanism of protein phosphatases: insights into catalysis and regulation. Annu Rev Biophys Biomol Struct *27*, 133-164.

Bashaw, G. J., Hu, H., Nobes, C. D., and Goodman, C. S. (2001). A novel Dbl family RhoGEF promotes Rho-dependent axon attraction to the central nervous system midline in *Drosophila* and overcomes Robo repulsion. J Cell Biol *155*, 1117-1122.

Billuart, P., Winter, C. G., Maresh, A., Zhao, X., and Luo, L. (2001). Regulating axon branch stability: the role of p190 RhoGAP in repressing a retraction signaling pathway. Cell *107*, 195-207.

Bilwes, A. M., den Hertog, J., Hunter, T., and Noel, J. P. (1996). Structural basis for inhibition of receptor protein-tyrosine phosphatase α by dimerization. Nature *382*, 555-559.

Blanchetot, C., and den Hertog, J. (2000). Multiple interactions between receptor protein-tyrosine phosphatase (RPTP) α and membrane-distal protein-tyrosine phosphatase domains of various RPTPs. J Biol Chem *275*, 12446-12452.

Brand, A. H., and Perrimon, N. (1993). Targeted gene expression as a means of altering cell fates and generating dominant phenotypes. Development *118*, 401-415.

Brose, K., Bland, K. S., Wang, K. H., Arnott, D., Henzel, W., Goodman, C. S., Tessier-Lavigne, M., and Kidd, T. (1999). Slit proteins bind Robo receptors and have an evolutionarily conserved role in repulsive axon guidance. Cell *96*, 795-806.

Denu, J. M., Lohse, D. L., Vijayalakshmi, J., Saper, M. A., and Dixon, J. E. (1996). Visualization of intermediate and transition-state structures in protein-tyrosine phosphatase catalysis. Proc Natl Acad Sci U S A *93*, 2493-2498.

Desai, C. J., Gindhart, J. G., Jr., Goldstein, L. S., and Zinn, K. (1996). Receptor tyrosine phosphatases are required for motor axon guidance in the *Drosophila* embryo. Cell *84*, 599-609.

Desai, C. J., Krueger, N. X., Saito, H., and Zinn, K. (1997). Competition and cooperation among receptor tyrosine phosphatases control motoneuron growth cone guidance in *Drosophila*. Development *124*, 1941-1952.

Desai, C. J., Popova, E., and Zinn, K. (1994). A *Drosophila* receptor tyrosine phosphatase expressed in the embryonic CNS and larval optic lobes is a member of the set of proteins bearing the "HRP" carbohydrate epitope. J Neurosci *14*, 7272-7283.

Desai, D. M., Sap, J., Schlessinger, J., and Weiss, A. (1993). Ligand-mediated negative regulation of a chimeric transmembrane receptor tyrosine phosphatase. Cell *73*, 541-554.

Dunn, D., Chen, L., Lawrence, D. S., and Zhang, Z. Y. (1996). The active site specificity of the Yersinia protein-tyrosine phosphatase. J Biol Chem *271*, 168-173.

Edwards, K. A., and Kiehart, D. P. (1996). *Drosophila* non-muscle myosin II has multiple essential roles in imaginal disc and egg chamber morphogenesis. Development *122*, 1499-1511.

Ferrari, D. M., and Soling, H. D. (1999). The protein disulphide-isomerase family: unravelling a string of folds. Biochem J *339 (Pt 1)*, 1-10.

Flint, A. J., Tiganis, T., Barford, D., and Tonks, N. K. (1997). Development of "substrate-trapping" mutants to identify physiological substrates of protein tyrosine phosphatases. Proc Natl Acad Sci USA *94*, 1680-1685.

Garton, A. J., Flint, A. J., and Tonks, N. K. (1996). Identification of p130(^{cas}) as a substrate for the cytosolic protein tyrosine phosphatase PTP-PEST. Mol Cell Biol *16*, 6408-6418.

Gross, S., Blanchetot, C., Schepens, J., Albet, S., Lammers, R., Den Hertog, J., and Hendriks, W. (2002). Multimerization of the protein-tyrosine phosphatase (PTP)-like

insulin-dependent diabetes mellitus autoantigens IA-2 and IA-2beta with receptor PTPs (RPTPs). Inhibition of RPTPα enzymatic activity. J Biol Chem *277*, 48139-48145.

Guan, K. L., and Dixon, J. E. (1991). Evidence for protein-tyrosine-phosphatase catalysis proceeding via a cysteine-phosphate intermediate. J Biol Chem *266*, 17026-17030.

Hayano, T., and Kikuchi, M. (1995). Molecular cloning of the cDNA encoding a novel protein disulfide isomerase-related protein (PDIR). FEBS Lett *372*, 210-214.

Hoffmann, K. M., Tonks, N. K., and Barford, D. (1997). The crystal structure of domain 1 of receptor protein-tyrosine phosphatase μ. J Biol Chem *272*, 27505-27508.

Iversen, L. F., Moller, K. B., Pedersen, A. K., Peters, G. H., Petersen, A. S., Andersen, H. S., Branner, S., Mortensen, S. B., and Moller, N. P. (2002). Structure determination of T cell protein-tyrosine phosphatase. J Biol Chem *277*, 19982-19990.

Jia, Z., Barford, D., Flint, A. J., and Tonks, N. K. (1995). Structural basis for phosphotyrosine peptide recognition by protein tyrosine phosphatase 1B. Science *268*, 1754-1758.

Jiang, G., den Hertog, J., and Hunter, T. (2000). Receptor-like protein tyrosine phosphatase α homodimerizes on the cell surface. Mol Cell Biol *20*, 5917-5929.

Jiang, G., den Hertog, J., Su, J., Noel, J., Sap, J., and Hunter, T. (1999). Dimerization inhibits the activity of receptor-like protein-tyrosine phosphatase-α. Nature *401*, 606-610.

Keleman, K., Rajagopalan, S., Cleppien, D., Teis, D., Paiha, K., Huber, L. A., Technau, G. M., and Dickson, B. J. (2002). Comm sorts robo to control axon guidance at the *Drosophila* midline. Cell *110*, 415-427.

Kidd, T., Bland, K. S., and Goodman, C. S. (1999). Slit is the midline repellent for the robo receptor in *Drosophila*. Cell *96*, 785-794.

Kolodziej, P. A., Timpe, L. C., Mitchell, K. J., Fried, S. R., Goodman, C. S., Jan, L. Y., and Jan, Y. N. (1996). *frazzled* encodes a *Drosophila* member of the DCC

immunoglobulin subfamily and is required for CNS and motor axon guidance. Cell *87*, 197-204.

Krueger, N. X., Van Vactor, D., Wan, H. I., Gelbart, W. M., Goodman, C. S., and Saito, H. (1996). The transmembrane tyrosine phosphatase DLAR controls motor axon guidance in *Drosophila*. Cell *84*, 611-622.

Lim, K. L., Kolatkar, P. R., Ng, K. P., Ng, C. H., and Pallen, C. J. (1998). Interconversion of the kinetic identities of the tandem catalytic domains of receptor-like protein-tyrosine phosphatase PTPα by two point mutations is synergistic and substrate-dependent. J Biol Chem *273*, 28986-28993.

Majeti, R., Bilwes, A. M., Noel, J. P., Hunter, T., and Weiss, A. (1998). Dimerization-induced inhibition of receptor protein tyrosine phosphatase function through an inhibitory wedge. Science *279*, 88-91.

Mansfield, S. G., al-Shirawi, D. Y., Ketchum, A. S., Newbern, E. C., and Kiehart, D. P. (1996). Molecular organization and alternative splicing in zipper, the gene that encodes the *Drosophila* non-muscle myosin II heavy chain. J Mol Biol *255*, 98-109.

Meng, K., Rodriguez-Pena, A., Dimitrov, T., Chen, W., Yamin, M., Noda, M., and Deuel, T. F. (2000). Pleiotrophin signals increased tyrosine phosphorylation of beta beta-catenin through inactivation of the intrinsic catalytic activity of the receptor-type protein tyrosine phosphatase beta/zeta. Proc Natl Acad Sci U S A *97*, 2603-2608.

Mishra-Gorur, K., and Castellot, J. J., Jr. (1999). Heparin rapidly and selectively regulates protein tyrosine phosphorylation in vascular smooth muscle cells. J Cell Physiol *178*, 205-215.

Mitchell, K. J., Doyle, J. L., Serafini, T., Kennedy, T. E., Tessier-Lavigne, M., Goodman, C. S., and Dickson, B. J. (1996). Genetic analysis of Netrin genes in *Drosophila*: Netrins guide CNS commissural axons and peripheral motor axons. Neuron *17*, 203-215.

Myat, A., Henry, P., McCabe, V., Flintoft, L., Rotin, D., and Tear, G. (2002). *Drosophila* Nedd4, a ubiquitin ligase, is recruited by Commissureless to control cell surface levels of the roundabout receptor. Neuron *35*, 447-459.

Nam, H. J., Poy, F., Krueger, N. X., Saito, H., and Frederick, C. A. (1999). Crystal structure of the tandem phosphatase domains of RPTP LAR. Cell *97*, 449-457.

Redowicz, M. J. (2001). Regulation of non-muscle myosins by heavy chain phosphorylation. J Muscle Res Cell Motil *22*, 163-173.

Rothberg, J. M., Jacobs, J. R., Goodman, C. S., and Artavanis-Tsakonas, S. (1990). Slit: an extracellular protein necessary for development of midline glia and commissural axon pathways contains both EGF and LRR domains. Genes Dev *4*, 2169-2187.

Schindelholz, B., Knirr, M., Warrior, R., and Zinn, K. (2001). Regulation of CNS and motor axon guidance in *Drosophila* by the receptor tyrosine phosphatase DPTP52F. Development *128*, 4371-4382.

Seeger, M., Tear, G., Ferres-Marco, D., and Goodman, C. S. (1993). Mutations affecting growth cone guidance in *Drosophila*: genes necessary for guidance toward or away from the midline. Neuron *10*, 409-426.

Streuli, M., Krueger, N. X., Thai, T., Tang, M., and Saito, H. (1990). Distinct functional roles of the two intracellular phosphatase like domains of the receptor-linked protein tyrosine phosphatases LCA and LAR. Embo J *9*, 2399-2407.

Stronach, B. E., and Perrimon, N. (2001). Investigation of leading edge formation at the interface of amnioserosa and dorsal ectoderm in the *Drosophila* embryo. Development *128*, 2905-2913.

Sun, Q., Bahri, S., Schmid, A., Chia, W., and Zinn, K. (2000). Receptor tyrosine phosphatases regulate axon guidance across the midline of the *Drosophila* embryo. Development *127*, 801-812.

Sun, Q., Schindelholz, B., Knirr, M., Schmid, A., and Zinn, K. (2001). Complex genetic interactions among four receptor tyrosine phosphatases regulate axon guidance in *Drosophila*. Mol Cell Neurosci *17*, 274-291.

Tertoolen, L. G., Blanchetot, C., Jiang, G., Overvoorde, J., Gadella, T. W., Jr., Hunter, T., and den Hertog, J. (2001). Dimerization of receptor protein-tyrosine phosphatase α in living cells. BMC Cell Biol *2*, 8.

Tian, S. S., Tsoulfas, P., and Zinn, K. (1991). Three receptor-linked protein-tyrosine phosphatases are selectively expressed on central nervous system axons in the *Drosophila* embryo. Cell *67*, 675-680.

Tsujikawa, K., Kawakami, N., Uchino, Y., Ichijo, T., Furukawa, T., Saito, H., and Yamamoto, H. (2001). Distinct functions of the two protein tyrosine phosphatase domains of LAR (leukocyte common antigen-related) on tyrosine dephosphorylation of insulin receptor. Mol Endocrinol *15*, 271-280.

Wallace, M. J., Fladd, C., Batt, J., and Rotin, D. (1998). The second catalytic domain of protein tyrosine phosphatase delta (PTP delta) binds to and inhibits the first catalytic domain of PTP sigma. Mol Cell Biol *18*, 2608-2616.

Winter, C. G., Wang, B., Ballew, A., Royou, A., Karess, R., Axelrod, J. D., and Luo, L. (2001). *Drosophila* Rho-associated kinase (Drok) links Frizzled-mediated planar cell polarity signaling to the actin cytoskeleton. Cell *105*, 81-91.

Young, P. E., Richman, A. M., Ketchum, A. S., and Kiehart, D. P. (1993). Morphogenesis in *Drosophila* requires non-muscle myosin heavy chain function. Genes Dev *7*, 29-41.

Zhang, Z. Y., Maclean, D., McNamara, D. J., Sawyer, T. K., and Dixon, J. E. (1994a). Protein tyrosine phosphatase substrate specificity: size and phosphotyrosine positioning requirements in peptide substrates. Biochemistry *33*, 2285-2290.

Zhang, Z. Y., Wang, Y., and Dixon, J. E. (1994b). Dissecting the catalytic mechanism of protein-tyrosine phosphatases. Proc Natl Acad Sci U S A *91*, 1624-1627.

Zhao, D. B., Cote, S., Jahnig, F., Haller, J., and Jackle, H. (1988). Zipper encodes a putative integral membrane protein required for normal axon patterning during *Drosophila* neurogenesis. Embo J *7*, 1115-1119.